Inorganic Chemistry

Article

pubs.acs.org/IC

Pt−Mo and Pt−W Mixed-Metal Clusters with Chelating or Bridging Diphosphine Short-Bite Ligands $(Ph_2P)_2NH$ and $(Ph_2P)_2N(CH_2)_9CH_3$: A Combined Synthetic and Theoretical Study

Stefano Todisco,[†] Vito Gallo,[†] Piero Mastrorilli,*[,†,‡] Mario Latronico,[†,‡] Nazzareno Re,[§] Francesco Creati,[§] and Pierre Braunstein*[,⊥]

[†]Dipartimento di Ingegneria Civile, Ambientale, del Territorio, Edile e di Chimica (DICATECh), Politecnico di Bari, via Orabona 4, I-70125 Bari, Italy

[‡]Consiglio Nazionale delle Ricerche, Istituto di Chimica dei Composti Organometallici (ICCOM-CNR), Via Orabona 4, 70125 Bari, Italy

[§]Dipartimento di Scienze del Farmaco, Università "G. d'Annunzio", Via dei Vestini 31, 06100 Chieti, Italy

[⊥]Laboratoire de Chimie de Coordination, UMR 7177 CNRS, Université de Strasbourg, 4 rue Blaise Pascal, CS 90032, F-67081 Strasbourg, France

Supporting Information

ABSTRACT: The reactivity of the complexes $[PtCl_2\{Ph_2PN(R)PPh_2\text{-}P,P\}]$ (R = −H, **3**; R = $-(CH_2)_9CH_3$, **8**) toward group 6 carbonylmetalates $Na[MCp(CO)_3]$ (M = W or Mo, Cp = cyclopentadienyl) was explored. When R = H, the triangular clusters $[PtM_2Cp_2(CO)_5(\mu\text{-dppa})]$ (M = W, **4**; M = Mo, **5**), in which the diphosphane ligand bridges a Pt-M bond, were obtained as the only products. When R = $-(CH_2)_9CH_3$, isomeric mixtures of the triangular clusters $[PtM_2Cp_2(CO)_5\{Ph_2PN(R)PPh_2\text{-}P,P\}]$, in which the diphosphane ligand chelates the Pt center (M = W, **11**; M = Mo, **13**) or bridges a Pt−M bond (M = W, **12**; M = Mo, **14**), were obtained. Irrespective of the M/Pt ratio used when R = $-(CH_2)_9CH_3$, the reaction of $[PtCl_2\{Ph_2PN(R)PPh_2\text{-}P,P\}]$ with $Na[MCp(CO)_3]$ in acetonitrile stopped at the mono-substitution stage with the formation of $[PtCl\{MCp(CO)_3\}\{Ph_2PN(R)PPh_2\text{-}P,P\}]$ (R = $-(CH_2)_9CH_3$, M = W, **9**; M = Mo, **10**), which are the precursors to the trinuclear clusters formed in THF when excess carbonylmetalate was used. The dynamic behavior of the dppa derivatives **4** and **5** in solution as well as that of their carbonylation products **6** and **7**, respectively, is discussed. Density functional calculations were performed to study the thermodynamics of formation of **4** and **5** and **11**−**14**, to evaluate the relative stabilities of the chelated and bridged forms and to trace a possible pathway for the formation of the trinuclear clusters.

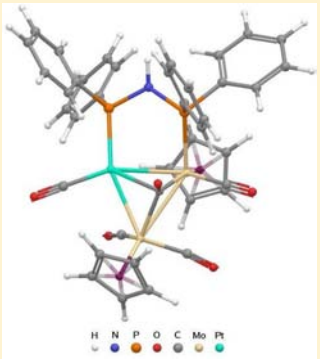

INTRODUCTION

Owing to its diversity, fundamental interest, and range of applications, the coordination chemistry of short-bite ligands such as dppm [dppm = bis(diphenylphosphanyl)methane] and dppa [dppa = bis(diphenylphosphanyl)amine] continues to attract considerable interest in the chemical community.[1] A particularly debated point deals with the conditions for the occurrence of the different coordination modes exhibited by these ligands: monodentate, chelating, or bridging. The presence and the nature of substituents on the spacer atom that separates the two P donors can affect the coordination mode of these ligands. It is known, for example, that the replacement of one or both hydrogen atoms of the dppm methylene group with an alkyl group results in a decrease of the P−C−P angle (Thorpe−Ingold or "gem-effect") and in a greater tendency to form stable chelates.[2]

In metal cluster complexes, such short-bite ligands can potentially exhibit any of the three bonding modes mentioned above and the first example of a heterodinuclear complex containing both bridging and chelating dppm ligands was observed in Pt−Mo chemistry.[3] Transformation of a chelating into a bridging dppm is favored by the enhanced stability of a five-membered compared to a four-membered ring structure, and this property has been used in mixed-metal cluster synthesis through carbonylmetalate-induced ring-opening reactions on $[PtCl_2(dppm\text{-}P,P)$ resulting in the formation of Pt−M(μ-dppm) moieties.[4] Structural isomers which differ by the bonding mode of such difunctional ligands are particularly interesting to study and can lead to a better insight into the parameters favoring a given bonding mode. Equilibria between such isomers are possible, in particular between the chelated and bridging forms of the ligand. Furthermore, dynamic exchange between the coordinated and dangling P ends of a monodentate dppm ligand has also been observed ("end-over end" mechanism).[5]

In mixed-metal $PtCo_2$ triangular clusters containing the dppa[6] or dppm[7] ligands, the short-bite ligand displays only a bridging

Received: July 4, 2012
Published: October 24, 2012

bonding mode. However, when going from dppa to *N*-substituted ligands in $[PtCo_2(CO)_7\{Ph_2PN(R)PPh_2\text{-}P,P\}]$ [R = $-CH_3$, $-(CH_2)_9CH_3$, $-(CH_2)_2S(CH_2)_5CH_3$, $-(CH_2)_2SCH_2C_6H_5$, C_6H_5], the tendency of the diphosphane ligand to chelate was found to increase with the bulkiness of the R substituent. Thus, for R = $-CH_3$, these clusters exist exclusively with a structure in which the diphosphane bridges two metal atoms, whereas two isomers (bridged and chelate, Scheme 1) form when R is a more sterically demanding group.[8]

Scheme 1. Structural Isomers of the $[PtCo_2(CO)_7\{Ph_2PN(R)PPh_2\text{-}P,P\}]$ Clusters As a Function of the R Group

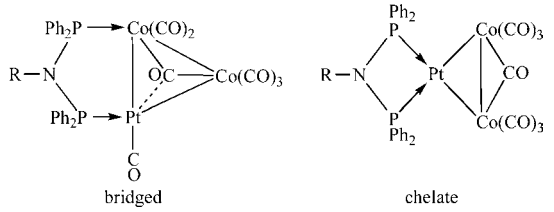

Triangular PtM_2 clusters of formula $[PtM_2Cp_2(CO)_5(dppm)]$ (Cp = cyclopentadienyl; M = W, **1**; M = Mo, **2**), prepared by reaction of $[PtCl_2(dppm\text{-}P,P)]$ with $[MCp(CO)_3]^-$ (M = Mo, W throughout the paper) are known to display only the bridged form of the diphosphane ligand,[4,7] as in the aforementioned dppm- or dppa-$PtCo_2$ clusters.[6,7] In order to evaluate a possible influence of the R substituent of diphenylphosphanyl amines in new PtW_2 or $PtMo_2$ clusters, we decided to investigate the reactivity of Pt(II) complexes of formula $[PtCl_2\{Ph_2PN(R)\text{-}PPh_2\text{-}P,P\}]$ [R = −H, $-(CH_2)_9CH_3$] toward the carbonylmetalates $[WCp(CO)_3]^-$ and $[MoCp(CO)_3]^-$.

RESULTS AND DISCUSSION

Clusters with the Ligand $(Ph_2P)_2NH$. The reactivity of $[PtCl_2(dppa\text{-}P,P)]$ (**3**) with $[MCp(CO)_3]^-$ parallels that found for $[PtCl_2(dppm\text{-}P,P)]$. Complex **3** reacted with 2 equiv $[MCp(CO)_3]^-$ in THF at 323 K to give, after 4 h, the triangular clusters $[PtM_2Cp_2(CO)_5(\mu\text{-dppa})]$ (M = W, **4**; M = Mo, **5**, Scheme 2), in ca. 80% isolated yield, which are analogous to **1**

Scheme 2. Synthesis of the $PtMo_2$ and PtW_2 Clusters

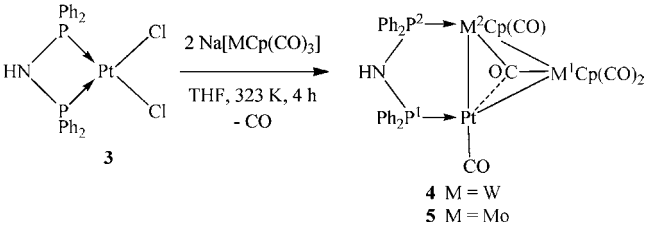

and **2**, respectively. Reaction time and temperature were optimized by taking into account the poor solubility of **3** in common solvents.[9] The latter explains that when the reactions were carried out with only 1 equiv of the carbonylmetalates, the same products were obtained, along with unreacted **3**.

The HRMS(−) spectrogram of cluster **4** showed a very intense peak at m/z = 1218.0296 corresponding to $[M - H]^-$, with an isotope pattern superimposable to that calculated on the basis of the proposed formula (Figure 1). The corresponding MS/MS spectrogram (see the Supporting Information (SI), Figure S1) contains peaks resulting from the loss of two, three or four CO ligands from **4**. In the positive mode, the HRMS spectrogram showed several peaks, including those corresponding to $[M + H]^+$ (1220.0384 da, calculated[10] 1220.0438 da), $[M + Na]^+$ (1242.0207 da, calculated 1242.0257 da) and $[2M + Na]^+$ (2459.0569 da, calculated 2459.0594 da). Similarly, the HRMS analyses of cluster **5** showed a peak at m/z = 1041.9398 corresponding to $[M - H]^-$ in negative mode (see SI, Figure S8), and peaks for $[M + H]^+$ (1043.9515 da, calculated 1043.9518 da), $[M + Na]^+$ (1065.9349 da, calculated 1065.9337 da), and $[2M + Na]^+$ (2107.8786 da, calculated 2107.8780 da) in positive mode.

NMR Studies. The $^{31}P\{^1H\}$ NMR spectrum of cluster **4** in CD_3CN (Figure 2) showed two mutually coupled doublets ($^2J_{P,P}$ = 48 Hz),[11] one at δ 60.6, flanked by two sets of satellites due to direct coupling with ^{195}Pt (isotopic abundance = 33.8%, $^1J_{P,Pt}$ = 4191 Hz) and to geminal coupling with $^{183}W^1$ (isotopic abundance = 14.3%, $^2J_{P,W}$ = 14 Hz) ascribed to the phosphorus atoms bonded to platinum (P^1), and one at δ 69.4 (P^2) flanked by two sets of satellites due to direct coupling with $^{183}W^2$ ($^1J_{P,W}$ = 350 Hz) and to coupling with ^{195}Pt ($^2J_{P,Pt}$ = 129 Hz). The $^{31}P\{^1H\}$ NMR resonances of the $PtMo_2$ cluster **5** (see SI, Figure S9) are deshielded with respect to the signals for **4**, falling at δ 66.8 (P^1) and δ 104.9 (P^2).

The $^{195}Pt\{^1H\}$ NMR spectra of **4** and **5** in CD_3CN (see SI, Figures S7 and S16) showed broad doublets of doublets centered at δ −3542 ($^1J_{Pt,P}$ = 4191 Hz, $^2J_{Pt,P}$ = 129 Hz, **4**) and δ −3490 ($^1J_{P,Pt}$ = 4309 Hz, $^2J_{P,Pt}$ = 130 Hz, **5**).

The ^1H NMR spectrum of **4** in CD_3CN showed, in addition to the resonances due to the phenyl protons in the range 7.0−7.9 ppm, a doublet of doublets at δ 6.80 flanked by ^{195}Pt satellites ($^2J_{H,P}$ = 2.3 Hz, $^2J_{H,P}$ = 5.1 Hz, $^3J_{H,Pt}$ = 126 Hz) attributable to the N−H proton, and two singlets at δ 5.35 and δ 5.21 for the cyclopentadienyl rings. The precise assignment of the latter resonances was made by means of $^1H-^{31}P$ HMQC experiments, which showed that each signal is scalar coupled to only one ^{31}P atom (see SI, Figure S2). Thus, the signal at δ 5.21, which is scalar coupled with P^2, corresponds to the Cp borne by the W^2 (bonded to P^2), while the signal at δ 5.35, which is coupled only with P^1, corresponds to the Cp borne by W^1.

The combined information stemming from $^1H-^{31}P$ HMQC and ^1H COSY spectra (see SI, Figure S3) also allowed the assignment of all the aromatic protons of **4**. In particular, the signals of the *ortho*-H (δ 7.84 and δ 7.03 for the phenyl rings bonded to P^1, δ 7.88 and δ 7.60 for the phenyl rings bonded to P^2) which belong to four inequivalent phenyl rings, could be identified. The inequivalence of the four phenyl rings can be explained by the unsymmetrical structure of the cluster resulting from the presence of the bridging CO. The latter is likely responsible for the broader $^{31}P\{^1H\}$ NMR signals of the isotopologue with ^{195}Pt. Indeed, the bridging CO generates an asymmetric environment around the Pt atom and this increases the chemical shift anisotropy contribution to the nuclear relaxation which, in turn, broadens the ^{195}Pt satellites (Figure 2).[12]

The $^{13}C\{^1H\}$ APT spectrum of **4** at 260 K in CD_3CN showed in the carbonyl region only three signals, all scalar coupled with ^{31}P and flanked by ^{183}W satellites at δ 230.6 (d, $J_{C,P}$ = 6 Hz, $^1J_{C-W}$ = 185 Hz), 233.5 (dd, $J_{C,P}$ = 8 and 3 Hz, $^1J_{C-W}$ = 122 Hz), and 242.4 (d, $J_{C,P}$ = 18 Hz, $^1J_{C-W}$ = 154 Hz) and which integrate approximately as 3:1:1 (see SI, Figure S5). None of them was flanked by ^{195}Pt satellites. Since for a given organometallic compound, the bridging carbonyls are deshielded with respect to terminal carbonyls,[13] we tentatively assign the signal at δ 242.4 to the bridging carbonyl and that at δ 233.5 to the carbonyl bonded

dx.doi.org/10.1021/ic301445h | *Inorg. Chem.* 2012, 51, 11549−11561

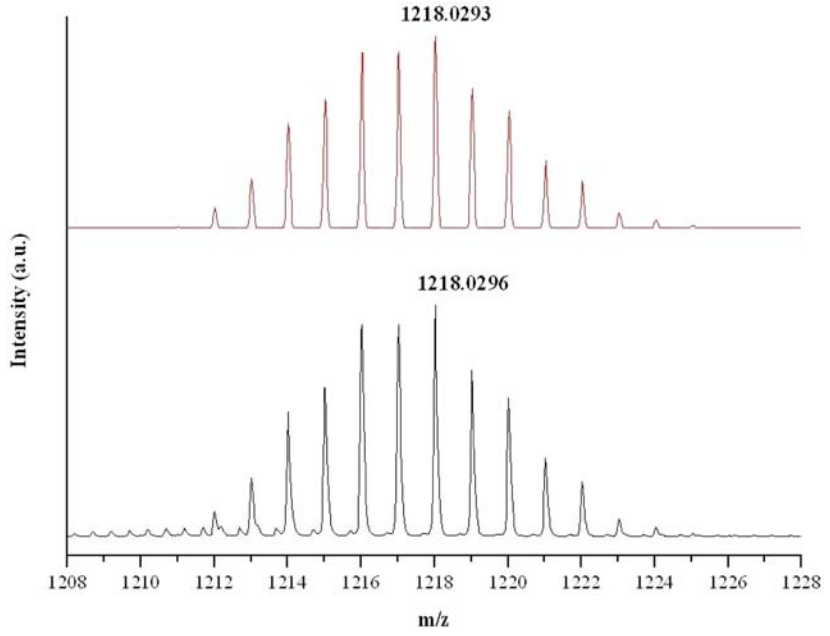

Figure 1. Experimental (bottom) and calculated (top) HRMS(−) spectrogram of **4** (exact mass =1218.0293 da) in THF/MeCN. The error between calculated and observed isotopic patterns is −0.3 ppm.

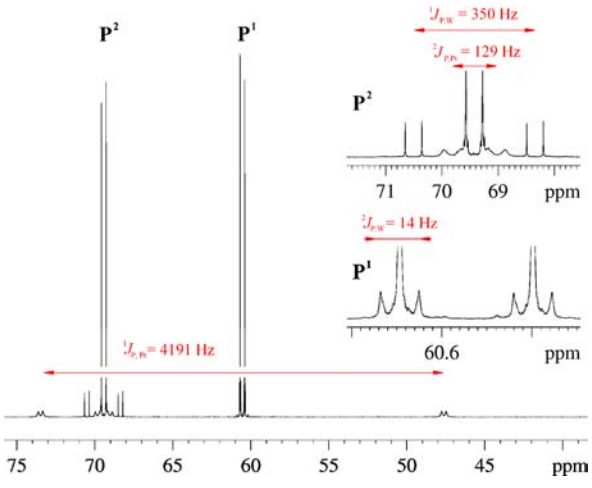

Figure 2. $^{31}P\{^{1}H\}$ NMR spectrum of **4** (161 MHz, 298 K, CD_3CN).

to W^2. The signal centered at δ 230.6 appears as a doublet flanked, beside the ^{183}W satellites, by two very broad peaks at δ 231.0 and δ 230.2 and it is interpreted as the averaged resonance of the two carbonyls bound to W^1 and of the carbonyl bound to the Pt, involved in a mutual exchange.[14] Recording the $^{13}C\{^{1}H\}$ APT spectra of **4** at 183 K resulted in a sharpening of the signals at δ 233.5 and δ 242.4, with contemporary broadening of the signal centered at δ 230.6.

The ^{1}H and $^{13}C\{^{1}H\}$ NMR features of **5** are quite similar to those of **4** and are reported in the Experimental Section.

*Dynamic Behavior of **4**−**5**.* The fluxional behavior of cluster **4** was investigated by multinuclear NMR EXSY experiments. No exchange was found in the $^{31}P\{^{1}H\}$ EXSY spectrum at 298 K, indicating the rigidity of the Pt−P−N−P−W core. Interestingly, the ^{1}H EXSY spectrum of **4** at 298 K (SI Figure S4) showed intense exchange cross peaks between the homologous signals of rings *A* and *B* bonded to P^1 and between the homologous signals of rings *C* and *D* bonded to P^2 (Scheme 3). For instance, the ortho protons of the phenyl ring *C* at δ 7.88 exchange with those of ring *D* at δ 7.60 while the ortho protons of the phenyl ring *A* at δ 7.03 exchange with those of ring *B* at δ 7.84. Since neither the cyclopentadienyl rings nor the P atoms participate in the exchange processes, the dynamic process resulting in the exchanges of rings *A*/*B* and *C*/*D* can be explained by a site exchange[15] between the bridging and a terminal carbonyl in the cluster, as shown in Scheme 3.

The exchange between the protons of rings *A*/*B* and *C*/*D* was also observed for the $PtMo_2$ cluster **5**, as evidenced by the ^{1}H EXSY spectrum (see SI, Figure S17).

Differently from the pairwise exchange of an even number of bridging carbonyls, for which many examples are reported,[14,16−22]

Scheme 3. Carbonyl Site Exchange for PtM_2 Clusters Accounting for the Exchange between the Protons of Rings *A*/*B* and *C*/*D*

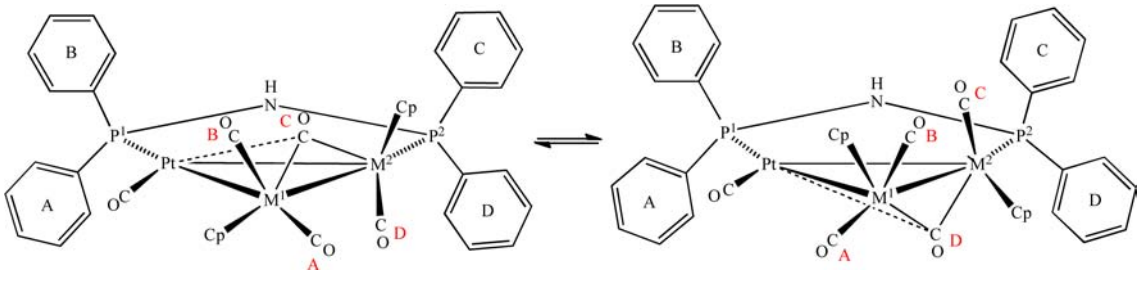

dx.doi.org/10.1021/ic301445h | *Inorg. Chem.* 2012, 51, 11549−11561

exchanges involving only one carbonyl bridge are less documented.[14,15b,23,24] In order to confirm the site exchange mechanism for the carbonyls in the dppa-PtM_2 clusters, we recorded a $^{13}C\{^1H\}$ EXSY spectrum of a CD_2Cl_2 solution of **4** at 258 K (Figure 3). It showed intense cross peaks between the

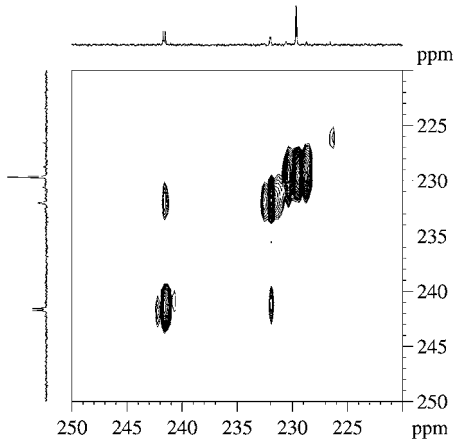

Figure 3. $^{13}C\{^1H\}$ EXSY spectrum of ^{13}CO enriched-**4** in CD_2Cl_2 at 258 K (carbonyl region).

signals at δ 231.9 (attributed to the terminal carbonyl on W^2) and at δ 241.7 (attributed to the carbonyl bridging W^1 and W^2). Analogous results were obtained from the $^{13}C\{^1H\}$ EXSY spectrum of **5** under similar conditions (see the SI, Figure S18), which showed intense cross peaks between the signals at δ 240.0 (attributed to the terminal carbonyl on Mo^2) and at δ 252.1 (attributed to the carbonyl bridging Mo^1 and Mo^2). These experiments can be interpreted in terms of the exchange between the carbonyls labeled C and D in Scheme 3, with associated movements of the cyclopentadienyls, and strongly support the occurrence of the carbonyl site exchange for **4** and **5**.

A deeper inspection of the $^{13}C\{^1H\}$ EXSY spectrum of **4** revealed that the diagonal peak due to the most shielded carbonyl signal (centered at δ 229.7 and attributed to the averaged resonances of the CO bonded to W^1 and Pt) is flanked by two intense peaks whose intensity and position do not correspond to those expected for ^{183}W satellites (Figure 3). Similar features were found in the $^{13}C\{^1H\}$ EXSY spectrum of the Mo_2Pt cluster **5** (see the SI, Figures S18 and S19) thus corroborating the assignment of the most shielded carbonyl signal for **4** and **5** to three carbonyl ligands involved in a complex dynamic process.

*Reversible Carbonylation of **4** and **5**.* In the IR spectra of the PtM_2 clusters in the solid state (ATR), the ν_{CO} absorptions were found at 1916, 1884, 1832, and 1770 cm^{-1} for **4** and at 1918, 1891, 1835, and 1779 cm^{-1} for **5**. These values are comparable with those reported for **1** (1911, 1887, 1836, 1775, 1754 cm^{-1}) and for **2** (1921, 1895, 1850, 1783, 1760 cm^{-1}).[7] The uptake of a CO molecule by **4** (or **5**) occurred when solutions of the clusters were exposed to an atmospheric pressure of CO at 298 K and resulted in the formation of the linear chain complexes **6** (or **7**); see Scheme 4.[25] The $PtMo_2$ cluster **5** was found more prone to carbonylation than **4**. Thus, exposing **5** to CO (p = 1 atm, T = 298 K) resulted invariably in quantitative carbonylation, irrespective of the solvent (dichloromethane, THF, acetonitrile, or toluene). Quantitative carbonylation of **4** into **6** was observed only when the reaction was carried out in aromatic solvents (toluene or C_6D_6), in which the solubility of CO is higher. The addition of CO is reversible and bubbling dinitrogen at room

Scheme 4. Reversible Carbonylation of the Triangular Clusters 4 and 5

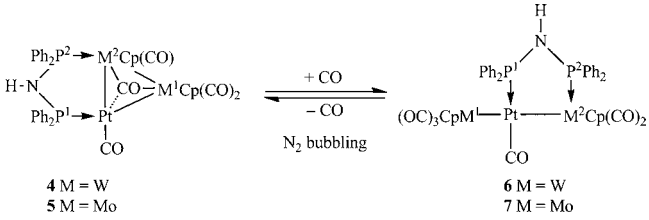

4 M = W
5 M = Mo

6 M = W
7 M = Mo

temperature through solutions of **6** or **7** was sufficient to remove one coordinated CO molecule and regenerate the triangular clusters **4** or **5**. This behavior is reminiscent of that observed with the analogous dppm-based clusters.[7]

Complex **6** was characterized by ^{13}C and ^{31}P NMR spectroscopy at low temperature since, at 298 K, the ^{31}P signals were very broad. The $^{31}P\{^1H\}$ NMR spectrum of a CD_2Cl_2 solution[26] of **4** and **6** under a ^{13}CO atmosphere at 258 K (see the SI, Figure S20) showed, in addition to the signals of **4**, two broad doublets ($^2J_{P,P}$ = 65 Hz) at δ 66.9 and δ 69.6 ascribed to **6**. The signal at δ 66.9 is flanked by ^{195}Pt satellites ($^1J_{P,Pt}$ = 3728 Hz) and is attributed to the P^1 atom bound to platinum while the signal at δ 69.6, flanked by ^{183}W satellites ($^1J_{P,W}$ = 336 Hz) (as well as ^{195}Pt satellites, $^2J_{P,Pt}$ = 215 Hz) is attributed to the phosphorus atom bound to W^2. The $^{13}C\{^1H\}$ APT spectrum of complex **6**, obtained upon reaction of **4** with ^{13}CO, was recorded under a ^{13}CO atmosphere in CD_2Cl_2 at 258 K and showed three signals at δ 207.4, δ 219.4, and δ 234.4. The former is a doublet ($^2J_{C,P}$ = 174 Hz) flanked by ^{195}Pt satellites ($^1J_{C,Pt}$ = 1436 Hz) and is assigned to the carbonyl directly bound to Pt in a trans position to P^1; the signal at δ 219.4 is a broad singlet flanked by ^{195}Pt satellites ($^2J_{C,Pt}$ = ca. 100 Hz) and ^{183}W satellites ($^1J_{C,W}$ = ca. 150 Hz) and is the averaged resonance of the carbonyls bonded to W^1. The signal at δ 234.4 is broad, flanked by ^{183}W satellites ($^2J_{C,W}$ = ca. 140 Hz), and is ascribed to the averaged resonances of the two carbonyls bonded to W^2. The $^{31}P\{^1H\}$ EXSY spectrum recorded at 258 K for the CD_2Cl_2 solution showed exchange cross peaks between the two ^{31}P signals of **6** (Figure 4).

Such an exchange can be explained by considering a CO shift from Pt to $W^2Cp(CO)_2$ with contemporary chelation of Pt by the diphosphane ligand (Scheme 5).

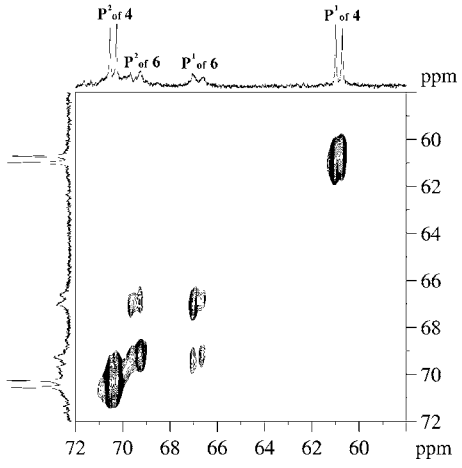

Figure 4. $^{31}P\{^1H\}$ EXSY spectrum of a mixture of **4** and **6** (CD_2Cl_2, 258 K).

dx.doi.org/10.1021/ic301445h | Inorg. Chem. 2012, 51, 11549−11561

Scheme 5. Proposed Fluxional Process of 6

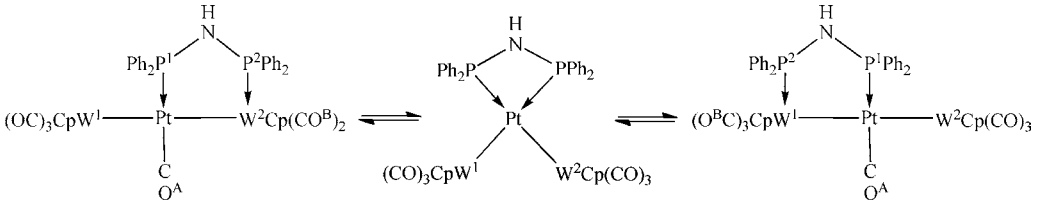

For the Mo analogue **7**, whose $^{31}P\{^1H\}$ and $^{13}C\{^1H\}$ signals are sharper than those of **6**, the $^{31}P\{^1H\}$ EXSY spectra did not reveal any exchange, even at 298 K (see the SI, Figure S22). The ^{195}Pt resonance for **6** and **7** was found at δ −4777 and δ −4443, respectively.

The HRMS(+) spectrogram of **6** and **7** showed intense peaks corresponding to the cation fragments resulting from loss of $[MCp(CO)_3]^-$.

Clusters with the Ligand $(Ph_2P)_2N(CH_2)_9CH_3$. The reactivity of the complex $[PtCl_2\{Ph_2PN(R)PPh_2\text{-}P,P\}]$ (R = $-(CH_2)_9CH_3$, **8**) differs from that of **3** since reaction of **8** with excess $[MCp(CO)_3]^-$ at 323 K in THF (or in CH_2Cl_2 or toluene) resulted in the formation of the chelate and bridged trinuclear clusters **11**−**12** (M = W) or **13**−**14** (M = Mo) as a mixture (Scheme 6). For the reaction carried out in THF, the isomeric ratios, assessed by ^{31}P integrals, were **11**/**12** = 1.6 (M = W) and **13**/**14** = 11 (M = Mo), indicating that chelation is the favored coordination mode for the *N*-decyl substituted ligand.

Scheme 6

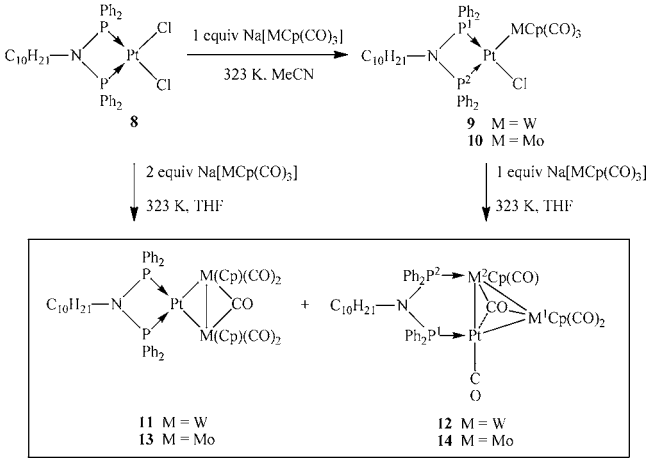

The heterotrinuclear clusters **11**−**14** are poorly stable and attempts to isolate them failed. The formation of isomeric trinuclear PtM_2 clusters (M = W, Mo) with chelating or bridging diphosphanes, parallels that observed for the analogous $PtCo_2$ clusters,[8] but in the present case, a thorough thermodynamic study was hampered by their extensive decomposition at temperatures higher than 313 K. However, the absence of an interconversion equilibrium between the two isomers could be ascertained by $^{31}P\{^1H\}$ EXSY experiments in the range 298−313 K.[27]

The chelated cluster **11** is characterized by a singlet in the $^{31}P\{^1H\}$ NMR at δ 45.8 with ^{195}Pt satellites ($^1J_{P,Pt}$ = 3101 Hz) and by a triplet at δ −4635 ($^1J_{P,Pt}$ = 3101 Hz) in the $^{195}Pt\{^1H\}$ NMR spectrum. The $^{31}P\{^1H\}$ NMR features of the bridged cluster **12** consist of two doublets ($^2J_{P,P}$ = 56 Hz) with ^{183}W and ^{195}Pt satellites centered at δ 86.6 ($^1J_{P,W}$ = 346 Hz, $^2J_{P,Pt}$ = 132 Hz) and δ 76.9 ($^2J_{P,W}$ = 12 Hz, $^1J_{P,Pt}$ = 4055 Hz). The former is assigned to P^2, directly bound to W, and the latter to P^1, which is directly bound to Pt. The $^{195}Pt\{^1H\}$ NMR spectrum of **12** showed a broad doublet at δ −3653 from which only the larger coupling constant $^1J_{P,Pt}$ = 4055 Hz could be extracted.

The ^1H EXSY spectrum of a CD_2Cl_2 solution of **12** or **14** at 298 K showed exchange cross peaks indicating, as already discussed for **4**, a site exchange between the single bridging and terminal carbonyl groups in the cluster. For instance, for complex **12**, clear cross peaks between the ortho protons of the phenyl rings bonded to P^2 (δ = 8.17 and 7.66, from the $^1H-^{31}P$ HMQC, Figure S30 in the SI) as well as between the ortho protons of the phenyl rings bonded to P^1 (δ = 7.82 and 7.46) were observed (see the SI, Figure S31).

The HRMS(+) spectrogram of MeCN/MeOH solutions of **11**/**12** (or **13**/**14**) showed intense peaks attributable to the ion $[M + H]^+$ (at 1360.2032 Da for M = W, at 1184.1066 Da for M = Mo), accompanied by peaks attributed to $[M + Na]^+$ (at 1382.1855 Da for M = W, at 1209.1087 Da for M = Mo), and $[2M + Na]^+$ (at 2739.3921 Da for M = W; at 2388.1959 Da for M = Mo).

Since complex **8** is soluble in organic solvents, it is possible to carry out the reaction by controlling the molar ratio of the reagents in solution. Thus, the reaction of **8** with exactly 1 equiv of $[MCp(CO)_3]^-$ at 323 K quantitatively led to the monosubstituted products $[PtCl\{MCp(CO)_3\}\{Ph_2PN(R)PPh_2\text{-}P,P\}]$ (M = W, **9**; M = Mo, **10**, Scheme 6). Given that addition of fresh $[MCp(CO)_3]^-$ to THF solutions of the bimetallic species **9** and **10** caused the formation of the corresponding triangular clusters **11** (or **13**) and **12** (or **14**), respectively, it is clear that the latter are formed via the intermediacy of the monosubstitution product **9** (or **10**).

Interestingly, when the reaction of **8** with $[MCp(CO)_3]^-$ was carried out in CH_3CN at 323 K, it stopped at the monosubstitution level, even when excess (>2 equiv) metalate was used.

Species analogous to **9** and **10**, of formula $[PtCl\{Co(CO)_4\}\{Ph_2PN(R)PPh_2\text{-}P,P\}]$ have been observed by NMR spectroscopy in reactions between $[PtCl_2\{Ph_2PN(R)PPh_2\text{-}P,P\}]$ and less than 2 equiv of $Na[Co(CO)_4]$[28] and a number of heterodinuclear Pt−Mo or Pt−W complexes of general formula $[PtR\{MCp(CO)_3\}(dppe\text{-}P,P)]$ have been recently reported.[29]

The $^{31}P\{^1H\}$ NMR spectrum of **9** in CD_3CN (see the SI, Figure S23) showed a doublet flanked by ^{195}Pt satellites at δ 51.6 (P *trans* to W, $^2J_{P,P}$ = 28 Hz, $^1J_{P,Pt}$ = 2583 Hz) and a doublet with ^{195}Pt and ^{183}W satellites at δ 26.6 (P *trans* to Cl, $^2J_{P,P}$ = 28 Hz, $^1J_{P,Pt}$ = 3571 Hz, $^2J_{P,W}$ = 12 Hz). The ^{31}P assignments, made on the basis of the $^1J_{P,Pt}$ values (with the larger value for the P^1 trans to Cl), were confirmed by the $^1H-^{31}P$ HMQC and ^1H NOESY spectra. Having assigned the ortho protons of the phenyl rings bonded to P^1 (δ 8.02) by $^1H-^{31}P$ HMQC spectra (see the SI, Figure S24), it was shown by a ^1H NOESY experiment (see the SI, Figure S25) that they are dipolar coupled to the cyclopentadienyl protons bound to W, thus confirming the spatial

dx.doi.org/10.1021/ic301445h | *Inorg. Chem.* 2012, 51, 11549−11561

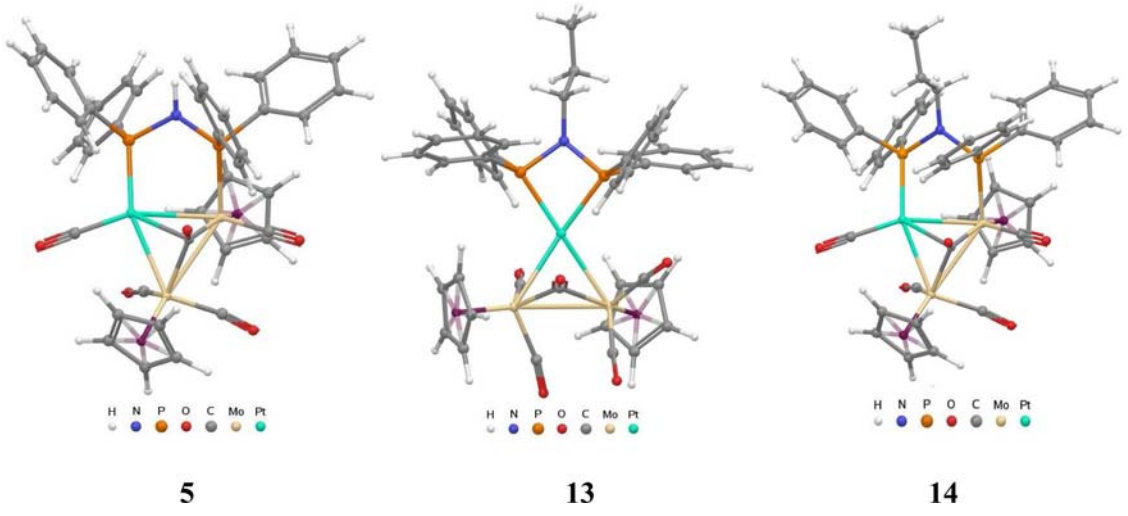

Figure 5. Calculated geometries of the $PtMo_2$ triangular clusters **5**, **13**, and **14**.

proximity of P^1 with W. The ^{31}P NMR features of **10** (see the SI, Figure S26) are similar to those of **9** and are reported in the Experimental Section. The $^{195}Pt\{^1H\}$ NMR spectrum of **9** (**10**) in CD_3CN showed a broad doublet of doublets centered at δ −4112 (δ −4014). While the ^{31}P NMR signals of **9** are quite sharp in acetonitrile at 298 K ($\Delta\nu_{1/2,P1}$ = 3 Hz, $\Delta\nu_{1/2,P2}$ = 24 Hz,) they consisted of a doublet with $\Delta\nu_{1/2,P2}$ = 53 Hz for P^2 and a very broad signal ($\Delta\nu_{1/2,P1}$ = 360 Hz for P^1) in THF at 298 K, which becomes sharper on lowering the temperature (the half-height width of the signals at 235 K were $\Delta\nu_{1/2,P1}$ = 8 Hz and $\Delta\nu_{1/2,P2}$ = 10 Hz). This suggests that in complex **9** at 298 K, the $WCp(CO)_3$ ligand may be partly dissociated in THF where an equilibrium may occur between the coordinated and the tight ion pair forms (for related solvent-induced heterolytic cleavage of Pd-M bonds, see ref 30). Such a behavior is corroborated by the slow exchange between P1 and P2 which was observed (^{31}P EXSY) for **9** in THF at 298 K, but was not observed either in THF at 235 K, or in MeCN at 298 K. Moreover, given that complexes **9** and **10** are dynamic in THF and not in MeCN, it may be argued that the subsequent reactivity with fresh $[MCp(CO)_3]^-$ is possible only for the ion pair present in THF.

The HRMS(+) spectrograms of acetonitrile solutions of **9** (or **10**) showed an intense peak attributable to the ion $[C_{42}H_{46}NO_3P_2PtM]^+$ (at 1052.2001 Da for M = W; at 966.1663 Da for M = Mo), which corresponds to $[M - Cl]^+$.

DFT Studies. Density functional calculations were performed to (i) provide plausible geometries for the trinuclear clusters **4**−**5** and **11**−**14**, supporting those proposed on the basis of HRMS and NMR data; (ii) to study the thermodynamics and trace a possible mechanism of their formation; and (iii) to evaluate the relative stabilities of their chelated and bridged forms. A preliminary study of the geometry and relative stabilities of the bridged and chelated isomers of the $[PtCo_2(CO)_7\{Ph_2PN(R)\text{-}PPh_2\text{-}P,P\}]$ clusters (R = CH_3, $(CH_2)_9CH_3$, $(CH_2)_2S(CH_2)_5CH_3$, $(CH_2)_2SCH_2C_6H_5$, C_6H_5) gave results in reasonable agreement with the experimental data,[8] suggesting that the employed M06/LACV3P++**//M06/LACVP* level of theory was sufficiently adequate to deal with such trinuclear clusters and the dppa bonding isomerization between chelating and bridging modes (Table 4). This study was carried out using models with *n*-propyl in place of the *n*-decyl group. For simplicity, we will not distinguish in the following discussion between the actual *n*-decyl substituted species and their *n*-propyl-substituted models.

We considered the PtM_2 (M = W, Mo) triangular clusters and performed geometry optimization on the dppa complexes **4** and **5** and their putative chelate isomers **4*** and **5*** as well as on the corresponding *N*-substituted analogues **11**−**14**. Several possible conformations were considered for each complex, differing mainly in the relative position of the carbonyl and cyclopentadienyl groups on M and only the global minima were subsequently taken into account. Since tungsten and molybdenum species have very similar structures, those for the $PtMo_2$ clusters **5**, **13**, and **14** are reported in Figure 5 whereas those for the PtW_2 clusters **4**, **11**, and **12** are reported as SI, Figure S34. In particular, the structures of **4** and **5** indicate a rigid Pt−P−N−P−M core and a *transoid* arrangement of the Cp ligands on the two M centers, consistent with the $^{31}P\{^1H\}$ and ^1H EXSY data discussed above.

In order to shed light on the formation of the triangular clusters deriving from reaction of **3** and **8** with $[MCp(CO)_3]^-$, we first considered the PtM (M = W, Mo) heterodinuclear complexes **9** and **10** and their putative unsubstituted dppa analogues, **9*** (Pt−W) and **10*** (Pt−Mo), possible intermediates in the monosubstitution of **3**. We found two possible isomers for each dinuclear complex, **A** and **B**, differing by the chelate or bridged coordination of the dppa ligand, respectively (Scheme 7).

The bridged isomers (**B**) of **9*** (Pt−W) and **10*** (Pt−Mo) were found lower in enthalpy with respect to the chelate ones (**A**) by 2.4 or 4.6 kcal mol^{-1}; see Figure 6 (1.4 and 2.6 kcal mol^{-1} in free energy, respectively, see Figure S35 in the SI) while the chelate isomers (**A**) of **9** (Pt−W) and **10** (Pt−W) are slightly lower in enthalpy for the *N*-substituted dppa species with respect to their putative bridged analogues by 2.4 or 0.6 kcal mol^{-1}, respectively, see Figure 7 (3.9 kcal mol^{-1} or 2.4 kcal mol^{-1} in free energy, see Figure S36, in the SI).

On the basis of these results and of all experimental data, we propose the reaction mechanism reported in Scheme 7. The first step consists of the nucleophilic substitution of the $[MCp(CO)_3]^-$ anion for a Cl^- ligand of **3** or **8** leading to the corresponding dinuclear PtMCl complexes **9***−**10*** or **9**−**10**. As discussed above, two possible isomers can be formed for each of these dinuclear species, **A** and **B**, corresponding to the chelate or bridged coordination of the diphosphanylamine.

It was then assumed that these monosubstituted complexes undergo a second nucleophilic substitution step whereby the remaining chloride ligand on Pt is replaced by the second

dx.doi.org/10.1021/ic301445h | *Inorg. Chem.* 2012, 51, 11549−11561

Scheme 7. Proposed Mechanism for the Formation of the Bridged and Chelated Trinuclear PtM_2 Clusters

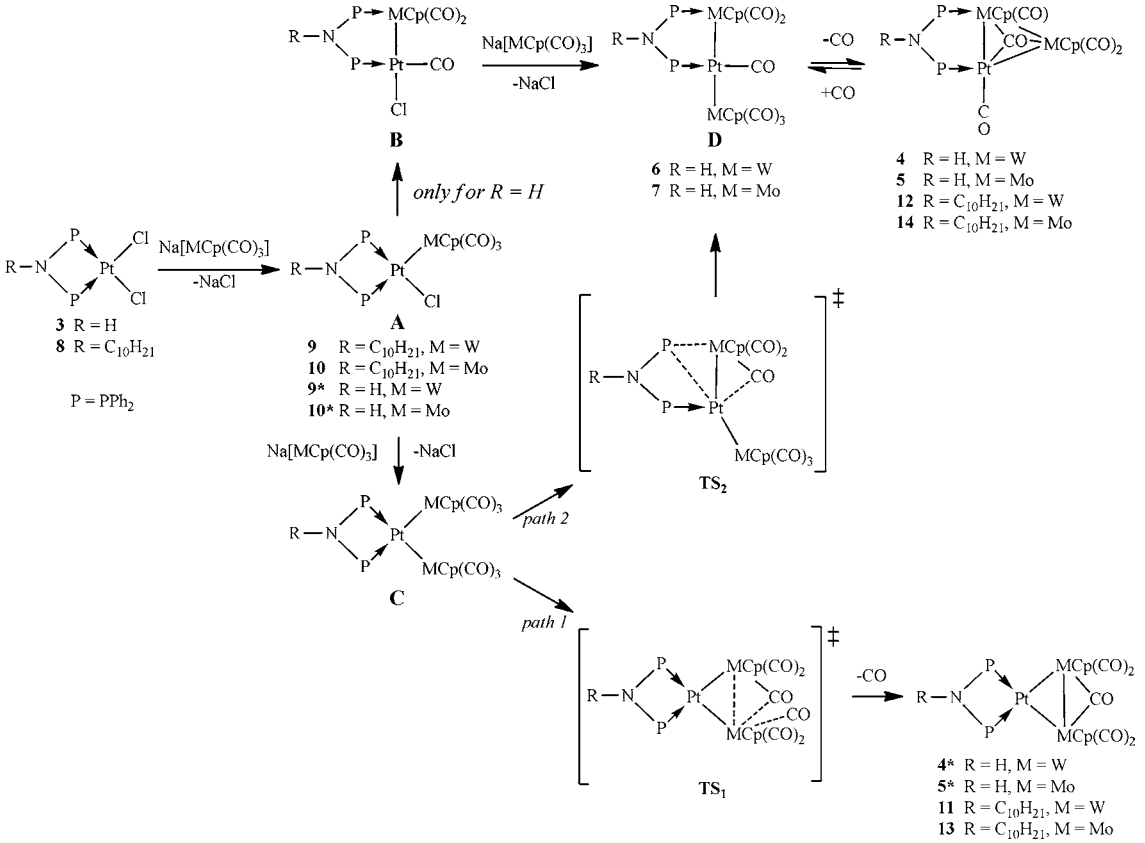

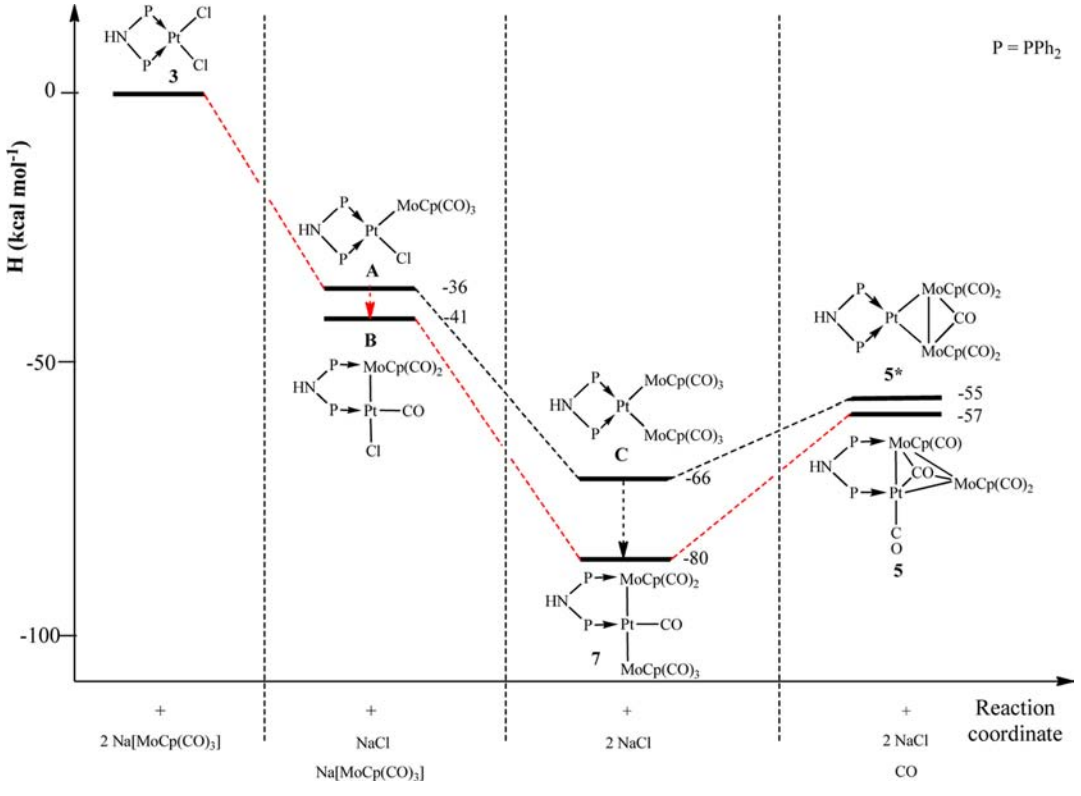

Figure 6. Enthalpy profile for the formation of the bridged and chelated trinuclear $PtMo_2$ clusters **5** and **5*** in THF solution.

$[MCp(CO)_3]^-$ anion. The second substitution on the bridged isomer **B** is expected to lead to a trinuclear chain complexes **D**, which were observed for R = −H (**6** and **7**, Scheme 4). Complexes **D** then lose a carbonyl group and form a M−M bond to give the final bridged clusters **4** and **5** (R = −H) or **12** and **14** [R = $-(CH_2)_9CH_3$].

dx.doi.org/10.1021/ic301445h | *Inorg. Chem.* 2012, 51, 11549−11561

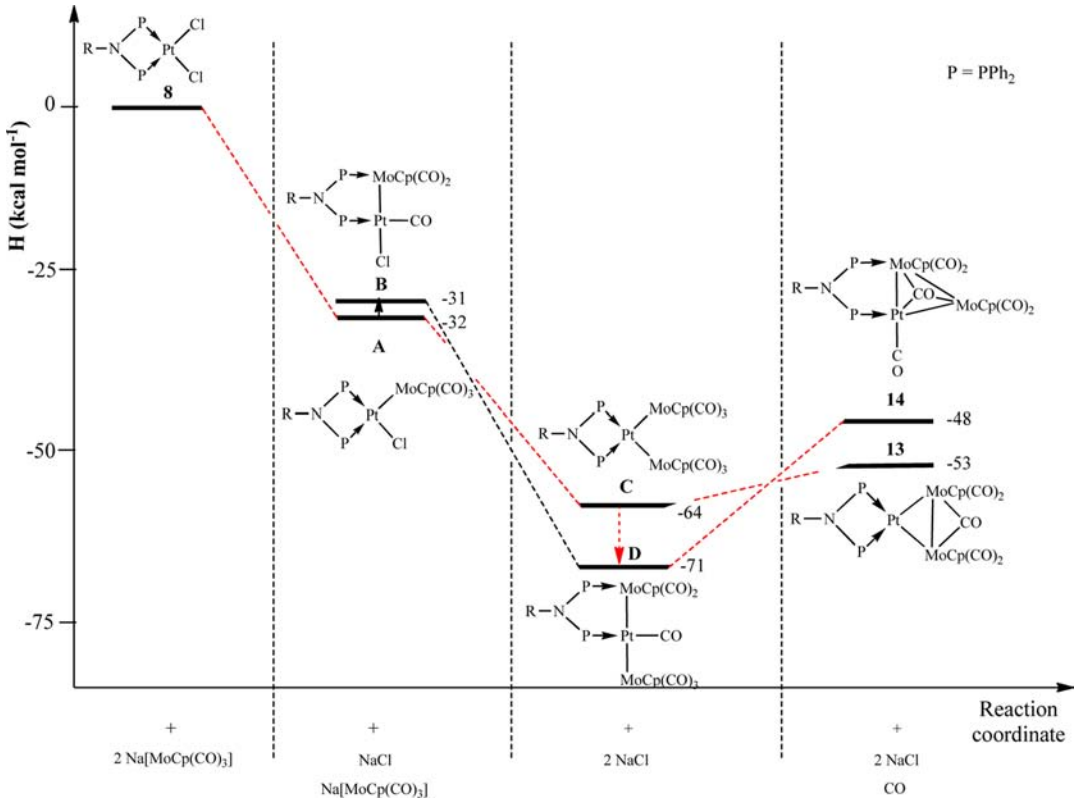

Figure 7. Enthalpy profile for the formation of the chelate and bridged trinuclear $PtMo_2$ clusters **13** and **14** [R = $-(CH_2)_9CH_3$] in THF solution.

The second substitution on the chelate isomer **A** is instead expected to lead to the trinuclear PtM_2 species **C** (not isolated). Their evolution may follow two different pathways: (i) formation of a M−M bond between the two *cis*-$MCp(CO)_3$ groups with loss of a carbonyl ligand and migration of a carbonyl to a bridging position, resulting in the final chelate clusters, **4*** and **5*** (R = −H, actually not observed), **11** and **13** [R = $-(CH_2)_9CH_3$, experimentally observed] (*path 1*); (ii) shift of one of the phosphorus atoms from Pt to the adjacent M atom, with simultaneous shift of a CO from the P-bonded M to the Pt center, leading to the linear chain complexes **D** which would then evolve to the final bridged clusters **4** and **5** (R = −H) or **12** and **14** [R = $-(CH_2)_9CH_3$] (*path 2*). This mechanism is supported by the following experimental data: (i) the reversible CO uptake by **4** and **5** leads to the chain complexes **6** and **7** (structure **D** in Scheme 7); (ii) the $^{31}P\{^1H\}$ EXSY spectrum shows exchange cross peaks between the two ^{31}P signals of **6**, which can be easily explained by a dynamic process involving the trinuclear open species **C**; see Scheme 5. A further support for this mechanism was gained by carrying out the reaction between **3** and 2 equiv of $Na[MoCp(CO)_3]$ in a sealed NMR tube (where the CO liberated cannot escape from the reaction mixture), which showed the contemporary formation of **5** and **7** (see the SI, Figure S33), thus substantiating the hypothesis that the linear chain complexes **D** are intermediate in the formation of the bridged clusters **4** and **5** (and therefore **12** and **14**).

We then calculated the thermodynamics of the formation of the final trinuclear complexes, **4** and **5** (R = −H) and **11**−**14** [R = $-(CH_2)_9CH_3$], from **3** or **8**, according to the mechanism proposed in Scheme 7. The relative enthalpies and free energies of the species involved in this mechanism are reported in Table 1, and the enthalpy profiles are shown for M = Mo and R = −H or $-(CH_2)_9CH_3$ in Figures 6 and 7, respectively (see the SI, Figures S35 and S36, showing the corresponding free energy profiles). It can be seen that both chloride substitution steps are exothermic and exoergonic and that the most stable species are the linear chain complexes of type **D**, the driving force for the formation of the triangular clusters being the entropic gain due to the loss of a CO molecule.

The relative stabilities of the chelate and bridged isomers of all considered trinuclear clusters are detailed in Table 2 in gas phase and in THF solution and show a little solvent effect, as expected from the similar polarity of the two isomers. For R = −H, the bridged isomers **4** or **5** are slightly more stable in enthalpy (ca. 2 kcal mol^{-1}) and almost isoenergetic in free energy with respect to the chelate ones **4*** or **5***. For the N-substituted dppa clusters, the chelate isomers are clearly more stable, both in enthalpy and free energy, by 4−8 kcal mol^{-1}. At first sight these results are not in complete agreement with the experimental data, as the experimental evidence shows that: (i) for R = −H only the bridged isomers **4** or **5** are observed while the calculations predict an equilibrium between bridged and chelate isomers; (ii) for R = $-(CH_2)_9CH_3$ both bridged **12** or **14** and chelate **11** or **13** isomers are actually observed while the calculations predict only the chelate ones. However, the NMR spectra indicate that the two isomers are not in equilibrium in solution so that the exact bridged to chelate ratio is determined by kinetic rather than thermodynamic factors, i.e. by the relative values of the highest barriers leading to them. Noteworthy, while for $PtCo_2$ clusters entropic factors were shown to govern the position of the bridged to chelate equilibrium,[8] for MPt_2 clusters a major role seems to be exerted by enthalpic contributions. This suggests that the higher stability found for the chelate forms on passing from dppa to $Ph_2PN(n\text{-}C_{10}H_{21})PPh_2$ in MPt_2 clusters may be due to a combination of electronic and steric effects exerted by the R substituent.

dx.doi.org/10.1021/ic301445h | *Inorg. Chem.* 2012, 51, 11549−11561

Table 1. Relative Enthalpies and Free Energies (kcal·mol^{-1}), in THF, of the Species Involved in the Formation of the Triangular Clusters $[PtM_2Cp_2(CO)_5\{Ph_2PN(R)PPh_2$-*P,P*$\}]$ (R = −H, $-(CH_2)_9CH_3$; M = Mo, W) with Respect to $[PtCl_2\{Ph_2PN(R)PPh_2$-*P,P*$\}]$ and $Na[MCp(CO)_3]$, Scheme 7

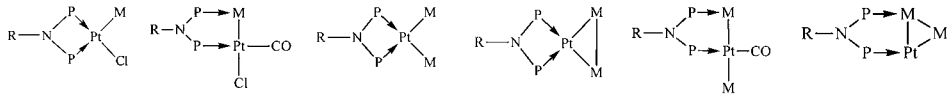

	A	B	C	D		
			Enthalpy			
M = Mo R = H	−35.9	−40.5	−66.2	−54.9	−79.5	−56.9
M = W R = H	−36.6	−39.0	−67.7	−53.7	−79.4	−55.0
M = Mo R= $C_{10}H_{21}$	−32.4	−31.8	−64.4	−53.3	−70.8	−47.8
M = W R = $C_{10}H_{21}$	−32.4	−30.0	−64.4	−52.5	−67.4	−43.1
			Free energy			
M = Mo R = H	−22.3	−24.9	−38.8	−39.3	−53.8	−40.2
M = W R = H	-24.3	−25.7	−40.4	−37.9	−51.1	−38.0
M = Mo R = $C_{10}H_{21}$	−20.4	−18.0	−38.7	−38.1	−40.7	−34.0
M = W R = $C_{10}H_{21}$	−22.2	−18.3	−38.5	−37.0	−41.5	−29.2

Table 2. Calculated Enthalpy and Free Energy (kcal·mol^{-1}) for the Bridged to Chelated Isomerization Process in the Triangular Clusters $[PtM_2Cp_2(CO)_5\{Ph_2PN(R)PPh_2$-*P,P*$\}]$ (R = −H, $-(CH_2)_9CH_3$; M = Mo, W) in the Gas Phase and in THF Solution

	gas phase		solution	
R	ΔH	ΔG	ΔH	ΔG
4 → **4*** (M = W, R = H)	+2.1	+1.0	+3.2	+0.6
5 → **5*** (M = Mo, R = H)	+3.7	+2.5	+1.8	+0.4
12 → **11** (M = W, R = $(CH_2)_9CH_3$)	−9.1	−7.5	−9.8	−8.2
14 → **13** (M = Mo, R = $(CH_2)_9CH_3$)	−7.2	−5.9	−5.7	−4.4

Due to the high computational load required to calculate the transition states for all the considered steps in Scheme 7, we could not face the kinetics of the proposed mechanism. However, some insight can be gained from the experimental evidence or from qualitative speculations. The easy occurrence of the substitution of the first chloride by a $[MCp(CO)_3]^-$ anion suggests a relatively low enthalpy barrier, below 25 kcal mol^{-1}, and an analogously low barrier is expected for the presumably similar substitution step of the second chloride ligands in **A** or **B** leading to **C** or **D**, respectively. A low barrier is expected for the evolution of **D** to the final bridged trinuclear cluster as suggested by the experimental evidence of an equilibrium between **6** (or **7**) and **4** (or **5**) in a sealed NMR tube (see above). More difficult to evaluate are the barriers for the evolution of **C** to the final bridged trinuclear cluster, paths 1 and 2 in Scheme 7, as both processes involve a more complex rearrangement. Indeed, path 1 involves the incipient formation of an M−M bond, the loss of a CO ligand, and the migration of a CO from a terminal to a bridging position, whereas path 2 involves the incipient breaking of a P−Pt bond, formation of a P−M bond, and migration of a carbonyl group (transition states $\mathbf{TS_1}$ and $\mathbf{TS_2}$ in Scheme 7). According to this picture, the bridged to chelate ratio would mainly be determined by the interplay between the **A** to **B** relative energies and the relative energy barriers of $\mathbf{TS_1}$ and $\mathbf{TS_2}$.

Figure 6 shows that for R = H, M = Mo, **B** is significantly lower in energy than **A**: the first Cl substitution in **3** would therefore lead almost exclusively to **B** which then, upon a second Cl substitution, leads to **D** (i.e., **7**) which finally evolves to the bridged trinuclear complex **5** explaining why this is the unique product. Similar considerations hold for the formation of **4**, with M = W; see Table 1.

Figure 7 shows that for R = $-(CH_2)_9CH_3$, M = Mo, **A** is slightly lower in energy than **B**: the first Cl substitution in **8** would therefore lead preferentially to **A** which then, upon a second Cl substitution, leads to **C** which may finally evolve to both the bridged (**14**) and chelate (**13**) trinuclear complexes, respectively, and the experimentally observed ratio is mainly determined by the relative energies of $\mathbf{TS_1}$ and $\mathbf{TS_2}$. Similar considerations hold for the formation of **11** and **12**, with M = W; see Table 1.

■ CONCLUSIONS

The reactivity of the carbonylmetalates $[MCp(CO)_3]^-$ (M = W, Mo) toward $[PtCl_2\{Ph_2PN(R)PPh_2$-*P,P*$\}]$ (R = H, $(CH_2)_9CH_3$) parallels that previously found for $[Co(CO)_4]^-$, although

dx.doi.org/10.1021/ic301445h | *Inorg. Chem.* 2012, 51, 11549−11561

significant differences are observed in the behavior of the products. In all cases, triangular PtM_2 (M = Co, Mo, or W) clusters were formed. For R = H, only the bridging coordination mode of the diphosphane ligand is observed while for R = $-(CH_2)_9CH_3$, both bridging and chelating coordination modes of the diphosphane occur. Whereas for the Co-based clusters with R = $-(CH_2)_9CH_3$, the bridged and chelate forms were found in equilibrium,[8] such an equilibrium could not be ascertained by NMR spectroscopy in the temperature range 298−323 K in the W- and Mo-based clusters. Moreover, the metal cores were found stable for all of the $PtCo_2$ and for PtM_2 (M = Mo, W) clusters with R = H, whereas for PtM_2 (M = Mo, W) with R = $-(CH_2)_9CH_3$, the triangular clusters were poorly stable and could not be isolated in the pure state.

DFT calculations applied to the mechanism of cluster formation indicate that the reaction starts with two subsequent replacements of $[MCp(CO)_3]^-$ for Cl^- ligands on Pt resulting in the linear trinuclear complexes $[Pt\{MCp(CO)_3\}_2\{Ph_2PN(R)PPh_2\text{-}P,P\}]$ in two different forms, bridged (**D**) for the dppa or chelate (**C**) for the *N*-alkyl dppa ligand. Species **D** may then evolve exclusively to the bridged form of the triangular clusters while species **C** may evolve by following two pathways, one leading to the chelate form of the triangular clusters and the other one leading to the linear chain complexes **D** which in turn loose a CO ligand to give the bridged form of the triangular clusters.

EXPERIMENTAL SECTION

All manipulations were conducted under an inert gas (argon) using standard Schlenk techniques. Solvents were dried and distilled under argon according to standard procedures. The complexes $[PtCl_2(dppa\text{-}P,P)]$ (**3**),[9] $[PtCl_2\{Ph_2PN(R)PPh_2\text{-}P,P\}]$ [R = $(CH_2)_9CH_3$],[8] and $Na[MCp(CO)_3]$ [M = Mo, W, as 1,2-dimethoxyethane (DME) solvates][31] were prepared by literature methods. ^{13}CO (ISOTEC Stable Isotopes) was purchased by Aldrich.

Multinuclear NMR spectra were recorded with a Bruker Avance 400 spectrometer (400 MHz for ^1H) at 298 K; chemical shifts are reported in parts per million referenced to $SiMe_4$ for ^1H and ^{13}C, H_3PO_4 for ^{31}P, and H_2PtCl_6 for ^{195}Pt. The signal attributions and coupling constant assessment was made on the basis of a multinuclear NMR analysis including, beside 1D spectra, $^{31}P\{^1H\}$ COSY, ^1H COSY, ^1H NOESY, $^1H-^{13}C$ HMQC, $^1H-^{13}C$ HMBC, $^1H-^{31}P$ HMQC, $^1H-^{195}Pt$ HMQC. The IR spectra were recorded with Bruker Vector 22 or Jasco FT-IR-4200 spectrometers. High resolution mass spectrometry (HRMS) and MS/MS analyses were performed using a time-of-flight mass spectrometer equipped with an electrospray ion source (Bruker micrOTOF-Q II). The analyses were carried out in a positive and in a negative ion mode. The sample solutions were introduced by continuous infusion with the aid of a syringe pump at a flowrate of 180 μL/h. The instrument was operated at end plate offset −500 V and capillary −4500 V. Nebulizer pressure was 0.3 bar (N_2), and the drying gas (N_2) flow was 4 L/min. Drying gas temperature was set at 453 K. The software used for the simulations is Bruker Daltonics Data Analysis (version 4.0). MS/MS analyses resulted in the fragmentation of the parent ion by loss of one, two, and three CO molecules. C, H, N elemental analyses were carried out with a Eurovector CHNS-O EA3000 Elemental Analyzer.

$[PtW_2Cp_2(CO)_5(\mu\text{-dppa})]$ (4). A THF solution of $Na[WCp(CO)_3]\cdot 2$ DME (156 mg, 0.292 mmol in 7.0 mL) was added in one portion to a stirred suspension of **3** in THF (95 mg, 0.146 mmol in 3.0 mL) kept at 323 K. The pale yellow suspension turned dark pink, and after it was stirred for 4 h, the mixture was cooled down to room temperature and the solvent was removed under reduced pressure. Toluene (20 mL) was added to the residue, and the resulting suspension was filtered. The filtrate was evaporated, and **4** was obtained as a fuchsia solid by crystallization from THF/*n*-hexane. Yield: 79%. Anal. calcd for $C_{39}H_{31}NO_5P_2PtW_2$: C 38.45, H 2.56, N 1.15; found C 38.83, H 2.59, N 1.14. HRMS(−), exact mass for the anion $[C_{39}H_{30}NO_5P_2PtW_2]^-$: 1218.0293; measured *m*/*z* 1218.0296 $(M-H)^-$. IR (ATR, cm^{-1}): 1916 (s), 1884 (vs), 1832 (s), 1801 (sh), 1770 (s). $^{31}P\{^1H\}$ NMR (CD_3CN, 298 K): δ 60.6 (d, $^2J_{P,P}$ = 48 Hz, $^1J_{P,Pt}$ = 4191 Hz, $^2J_{P,W}$ 14 Hz, P^1), δ 69.4 (d, $^2J_{P,P}$ = 48 Hz, $^1J_{P,W}$ = 350 Hz, $^2J_{P,Pt}$ 129 Hz, P^2). ^1H NMR (CD_3CN, 298 K): δ 5.21 (s, $C_5H_5-W^2$), δ 5.35 (s, $C_5H_5-W^1$), δ 6.80 (dd, $^2J_{H,P}$ 2.3 Hz, $^2J_{H,P}$ 5.1 Hz, $^3J_{H,Pt}$ 126 Hz, NH), ring A δ 7.03 (*o*), 7.10 (*m*), 7.21 (*p*); ring B δ 7.84 (*o*), 7.61 (*m*), 7.48 (*p*); ring C δ 7.88 (*o*), 7.47 (*m*), 7.58 (*p*); ring D δ 7.60 (*o*), 7.82 (*m*), 7.46 (*p*). $^{13}C\{^1H\}$ NMR (CD_3CN, 260 K): δ 242.4 (d, $J_{C,P}$ 18 Hz, $^1J_{C-W}$ = 165 Hz, CO), δ 233.5 (dd, $J_{C,P}$ = 8 and 3 Hz, $^1J_{C-W}$ = 165 Hz, CO), δ 230.6 (d, $J_{C,P}$ = 6 Hz, $^1J_{C-W}$ = 184 Hz, CO), δ 140.6 (d, $J_{C,P}$ = 50 Hz, C^{ipso}), δ 140.4 (dd, $J_{C,P}$ = 59 Hz, $J_{C,P}$ = 12 Hz, C^{ipso}), δ 137.0 (dd, $J_{C,P}$ = 65 Hz, $J_{C,P}$ = 5 Hz, C^{ipso}), δ 136.3 (dd, $J_{C,P}$ = 69 Hz, $J_{C,P}$ = 3 Hz, C^{ipso}), δ 134.0 (d, $J_{C,P}$ = 13 Hz, CH), δ 131.7 (d, $J_{C,P}$ = 13 Hz, CH), δ 131.6 (d, $J_{C,P}$ = 2 Hz, CH), δ 131.5 (d, $J_{C,P}$ = 3 Hz, CH), δ 131.2 (d, $J_{C,P}$ = 13 Hz, CH), δ 130.8 (d, $J_{C,P}$ = 3 Hz, CH), δ 130.6 (d, $J_{C,P}$ = 2 Hz, CH), δ 130.5 (d, $J_{C,P}$ = 10 Hz, CH),δ 129.3 (d, $J_{C,P}$ = 12 Hz, CH), δ 128.8 (d, $J_{C,P}$ = 11 Hz, CH),δ 128.7 (d, $J_{C,P}$ = 10 Hz, CH), δ 128.3 (d, $J_{C,P}$ = 12 Hz, CH), δ 91.8 (d, $J_{C,P}$ = 0.8 Hz, Cp−W^2), 88.7 (s, Cp−W^1).

$^{195}Pt\{^1H\}$ NMR (CD_3CN, 258 K): δ −3524 (dd, $^1J_{P,Pt}$ = 4191 Hz, $^2J_{P,Pt}$ = 129 Hz).

Synthesis of $[PtMo_2Cp_2(CO)_5(\mu\text{-dppa})]$ (5). A THF solution of $Na[MoCp(CO)_3]\cdot 2$DME (148 mg, 0.330 mmol in 7.0 mL) was added in one portion to a stirred suspension of **3** in THF (102 mg, 0.155 mmol in 3.0 mL) kept at 323 K. The pale yellow suspension turned violet and, after it was stirred for 4 h, the mixture was cooled down to room temperature and the solvent was removed under reduced pressure. Toluene (20 mL) was added to the residue, and the resulting suspension was filtered. The filtrate was evaporated, and **5** was obtained as a dark violet solid by crystallization from THF/*n*-hexane. Yield: 77%. Anal. calcd for $C_{39}H_{31}NO_5P_2PtMo_2$: C 44.93, H 3.00, N 1.34; found C 45.38, H 3.03, N 1.32. HRMS(−), exact mass for the anion $[C_{39}H_{30}Mo_2NO_5P_2Pt]^-$: 1041.9370; measured *m*/*z* 1041.9398 $(M-H)^-$. IR (ATR, cm^{-1}): 1918 (s), 1891 (vs), 1835 (s), 1807 (sh), 1779 (vs). $^{31}P\{^1H\}$ NMR (THF, 298 K): δ 66.8 (d, $^2J_{P,P}$ = 40 Hz, $^1J_{P,Pt}$ = 4309 Hz, P^1), δ 104.9 (d, $^2J_{P,P}$ = 40 Hz, $^2J_{P,Pt}$ 130 Hz, P^2). $^{195}Pt\{^1H\}$ NMR (CD_3CN, 298 K): δ −3490 (dd, $^1J_{P,Pt}$ = 4309 Hz, $^2J_{P,Pt}$ = 130 Hz). ^1H NMR (CD_3CN, 253 K): δ 5.23 (s, $C_5H_5-Mo^2$), δ 5.46 (s, $C_5H_5-Mo^1$), δ 6.73 (dd, $^2J_{H,P}$ 2.1 Hz, $^2J_{H,P}$ 5.9 Hz, $^3J_{H,Pt}$ 133 Hz, NH), ring A δ 7.14 (*o*), 7.26 (*m*), 7.37 (*p*); ring B δ 7.96 (*o*), 7.78 (*m*), 7.62 (*p*); ring C δ 7.99 (*o*), 7.63 (*m*), 7.77 (*p*); ring D δ 7.74 (*o*), 7.62 (*m*), 7.73 (*p*). $^{13}C\{^1H\}$ NMR (CD_3CN, 260 K): δ 253.5 (d, $J_{C,P}$ 27 Hz, CO), δ 241.4 (broad, CO), δ 239.6 (d, $J_{C,P}$ = 7 Hz, CO); δ 141.0 (dd, $J_{C,P}$ = 51 Hz, $J_{C,P}$ = 9 Hz, C^{ipso}), δ 141.1 (d, $J_{C,P}$ = 42 Hz, C^{ipso}), δ 138.1 (dd, $J_{C,P}$ = 66 Hz, $J_{C,P}$ = 6 Hz, C^{ipso}), δ 137.2 (dd, $J_{C,P}$ = 67 Hz, $J_{C,P}$ = 3 Hz, C^{ipso}), δ 134.0 (s, CH), δ 133.9 (s, CH), δ 132.5 (d, $J_{C,P}$ = 13 Hz, CH), δ 132.2 (d, $J_{C,P}$ = 13 Hz, CH), δ 132.1 (d, $J_{C,P}$ = 13 Hz, CH), δ 131.6 (s, CH), δ 131.1 (s, CH), δ 131.0 (d, $J_{C,P}$ = 11 Hz, CH), δ 129.9 (d, $J_{C,P}$ = 11 Hz, CH), δ 129.5 (d, $J_{C,P}$ = 10 Hz, CH), δ 129.4 (d, $J_{C,P}$ = 11 Hz, CH), δ 128.9 (d, $J_{C,P}$ = 12 Hz, CH), 93.8 (s, Cp), 91.0 (s, Cp).

Carbonylation of 4 and 5. In an NMR tube, a toluene (or CD_2Cl_2) solution of **4** (0.040 g, 0.033 mmol in 0.5 mL) was exposed to a pure CO (or ^{13}CO) atmosphere at room temperature and vigorously shaken. After 2 h (24 h in CD_2Cl_2), multinuclear NMR analysis revealed the quantitative transformation into **6** (spectroscopic yield >95%). The same procedure was followed using CD_3CN as solvent and a 24 h reaction time for the carbonylation of **5** to give **7**.

6. HRMS(+), exact mass for the cation $[C_{32}H_{26}NO_3P_2PtW]^+$ $(M-[W(CO)_3(Cp)])^+$: 912.0520; measured *m*/*z* 912.0560. IR (toluene, cm^{-1}): ν_{CO} 2020 (m), 1940 (vs), 1897 (vs), 1858 (s), 1856 (s). $^{31}P\{^1H\}$ NMR (CD_2Cl_2 268 K): δ 66.9 (d, $^2J_{P,P}$ = 65 Hz, $^1J_{P,Pt}$ = 3728 Hz, P−Pt), δ 69.6 (d, $^2J_{P,P}$ = 65 Hz, $^1J_{P,W}$ = 336 Hz, $^2J_{P,Pt}$ = 215 Hz, P−W). $^{13}C\{^1H\}$ NMR (CD_2Cl_2, 258 K, from the reaction with ^{13}CO): δ 234.4 (broad, $^1J_{C,W}$ = ca. 140 Hz, CO), δ 219.4 (broad, $^2J_{C,Pt}$ = 100 Hz, $^1J_{C,W}$ = ca. 150 Hz, CO), 207.4 (d, $^2J_{C,P}$ = 174 Hz, $^1J_{C,Pt}$ = 1436 Hz, CO). $^{195}Pt\{^1H\}$ NMR (C_6D_6, 298 K): δ −4777 (d, $^1J_{P,Pt}$ = 3774 Hz).

7. HRMS(+), exact mass for the cation $[C_{32}H_{26}NO_3P_2PtMo]^+$ $(M-[Mo(CO)_3(Cp)])^+$: 826.0066; measured *m*/*z* 826.0091. IR (toluene, cm^{-1}): ν_{CO} 2003 (m), 1940 (vs), 1899 (vs), 1845 (s), 1841 (s). $^{31}P\{^1H\}$ NMR (THF, 298 K): δ 65,8 (d, $^2J_{P,P}$ = 66 Hz, $^1J_{P,Pt}$ = 3740 Hz, P−Pt), δ 102.1 (d, $^2J_{P,P}$ = 66 Hz, $^2J_{P,Pt}$ 250 Hz, P−Mo). $^{13}C\{^1H\}$ NMR (CD_3CN,

dx.doi.org/10.1021/ic301445h | *Inorg. Chem.* 2012, 51, 11549−11561

260 K, from the reaction with ^{13}CO): δ 245.5 (d, $J_{C,P}$ = 23 Hz, CO), δ 227.3 (d, $J_{C,P}$ = 6 Hz, $J_{C,Pt}$ = 104 Hz, CO), δ 227.3 (dd, $J_{C,P}$ = 169 Hz, $J_{C,P}$ = 6 Hz, $J_{C,Pt}$ = 1418 Hz, CO). $^{195}Pt\{^1H\}$ NMR (CD_3CN, 283 K): δ −4443 (dd, $^1J_{P,Pt}$ = 3740 Hz, $^2J_{P,Pt}$ = 250 Hz).

Synthesis of the Monosubstituted Complexes 9 and 10. An acetonitrile solution of $Na[WCp(CO)_3]\cdot 2DME$ (83 mg, 0.155 mmol in 7.0 mL) was added dropwise to a stirred solution of **8** in acetonitrile (95 mg, 0.146 mmol in 3.0 mL) kept at 323 K. The pale yellow solution turned immediately orange, and after it was stirred for 1 h, the mixture was cooled and analyzed by NMR and HRMS that revealed the quantitative transformation into **9** (spectroscopic yield >95% based on ^{31}P integrals). Removal of the solvent and treatment with toluene in an attempt to purify the product resulted in partial conversion of **9** into **11**/**12** due to the slight excess of metalate used.

The same procedure was followed for the synthesis of **10**.

9. HRMS(+), exact mass for the cation $[C_{42}H_{46}NO_3P_2PtW]^+$ $(M-Cl)^+$: 1052.2085; measured m/z 1052.2001. $^{31}P\{^1H\}$ NMR (CD_3CN, 298 K): δ 51.6 (br, $^2J_{P,P}$ = 28 Hz, $^1J_{P,Pt}$ = 2583 Hz, P−Pt), δ 26.6 (d, $^2J_{P,P}$ = 28 Hz, $^1J_{P,Pt}$ 3571 Hz, $^2J_{P,W}$ = 12 Hz). ^1H NMR (CD_3CN): δ 8.12−7.55 (m, 20H, phenyl), δ 4.72 (s, 5H, Cp), δ 2.78 (m, 2H, CH_2N) δ 1.35−0.61 (m, 19H, aliphatic). $^{195}Pt\{^1H\}$ NMR (CD_3CN, 298 K): δ −4112 (dd, $^1J_{P,Pt}$ = 3573 Hz, $^1J_{P,Pt}$ = 2582 Hz). IR (CH_3CN, cm^{-1}): ν_{CO} 1889 (vs), 1772 (vs).

10. HRMS(+), exact mass for the cation $[C_{42}H_{46}MoNO_3P_2Pt]^+$ $(M-Cl)^+$: 966.1654; measured: m/z: 966.1663. $^{31}P\{^1H\}$ NMR (CD_3CN, 298 K): δ 53.6 (br, $^2J_{P,P}$ = 28 Hz, $^1J_{P,Pt}$ = 2648 Hz, P−Pt), δ 28.4 (d, $^2J_{P,P}$ = 28 Hz, $^1J_{P,Pt}$ 3549 Hz). ^1H NMR (CD_3CN): δ 8.11−7.55 (m, 20H, phenyl), 4.68 (s, 5H, Cp), δ 2.79 (m, 2H, CH_2N) δ 1.39−0.51 (m, 19H, aliphatic). $^{195}Pt\{^1H\}$ NMR (CD_3CN, 298 K): δ −4014 (dd, $^1J_{P,Pt}$ = 3550 Hz, $^1J_{P,Pt}$ = 2650 Hz). IR (CH_3CN, cm^{-1}): ν_{CO} 1895(vs), 1776(vs).

Synthesis of $[PtW_2Cp_2(CO)_5\{C_{10}H_{21}N(PPh_2)_2\}]$ (11 and 12). A THF solution of $Na[WCp(CO)_3]\cdot 2DME$ (182 mg, 0.340 mmol in 25 mL) was added dropwise within 40 min to a stirred solution of **8** in THF (123 mg, 0.155 mmol in 3.0 mL) kept at 323 K. The pale yellow solution immediately darkened, and after it was stirred for 2 h, the mixture was cooled down to room temperature and the solvent was removed under reduced pressure. Toluene (40 mL) was added to the residue and the resulting suspension was filtered. The filtrate was concentrated at reduced pressure, and the resulting solution was analyzed by HRMS and NMR. HRMS(+), exact mass for the cation $[C_{49}H_{52}NO_5P_2PtW_2]^+$ $(M+H)^+$: 1360.2006; measured m/z 1360.2032.

11 + 12. $^{31}P\{^1H\}$ NMR (CD_3CN, 298 K): δ 45.8 (s, $^1J_{P,Pt}$ = 3101 Hz, **11**), δ 76.9 (d, $^2J_{P,P}$ = 56 Hz, $^1J_{P,Pt}$ = 4055 Hz, $^2J_{P,W}$ = 12 Hz, P^1, **12**), δ 86.6 (d, $^1J_{P,W}$ = 346 Hz, $^2J_{P,Pt}$ = 132 Hz, $^2J_{P,P}$ = 56 Hz, P^2, **12**). ^1H NMR (CD_3CN, 298 K): δ 8.42−7.28 (m, phenyls), δ 5.41 (s, Cp−W^2 of **12**), δ 5.37 (s, Cp−W^1 of **12**), δ 5.15 (s, Cp's of **11**), δ 3.03 (m, NCH_2, **12**), δ 2.61 (m, NCH_2, **11**), δ 1.58−0.48 (m, aliphatic). $^{195}Pt\{^1H\}$ NMR (THF, 298 K): δ −4635 (t, $^1J_{P,Pt}$ = 3101 Hz, **11**), δ −3653 (broad d, $^1J_{P,Pt}$ = 4055 Hz, **12**).

Synthesis of $[PtMo_2Cp_2(CO)_5\{C_{10}H_{21}N(PPh_2)_2\}]$ (13 and 14). A THF solution of $Na[MoCp(CO)_3]\cdot 2DME$ (139 mg, 0.310 mmol in 25 mL) was added dropwise within 40 min to a stirred solution of **8** in THF (115 mg, 0.145 mmol in 3.0 mL) kept at 323 K. The pale yellow solution immediately darkened, and after it was stirred for 2 h, the mixture was cooled down to room temperature and the solvent was removed under reduced pressure. Toluene (40 mL) was added to the residue, and the resulting suspension was filtered. The filtrate was concentrated at reduced pressure, and the resulting solution was analyzed by HRMS and NMR. HRMS(+), exact mass for the cation $[C_{49}H_{52}Mo_2NO_5P_2Pt]^+$ $(M+H)^+$: 1184.1084; measured m/z 1184.1066. $^{31}P\{^1H\}$ NMR (CD_2Cl_2, 298 K): δ 58.2 (s, $^1J_{P,Pt}$ = 3190 Hz, **13**), δ 84.2 (d, $^2J_{P,P}$ = 43 Hz, $^1J_{P,Pt}$ = 4236 Hz, P^1, **14**), δ 120.7 (d, $^2J_{P,P}$ = 43 Hz, $^2J_{P,Pt}$ = 138 Hz, P^2, **14**). ^1H NMR (CD_2Cl_2, 298 K): δ 8.29−7.16 (m, phenyls), δ 5.21 (s, Cp−Mo^2 of **14**), δ 5.16 (s, Cp−Mo^1 of **14**), δ 4.97 (s, Cp's of **13**), δ 2.75 (m, NCH_2, **14**), δ 2.56 (m, NCH_2, **13**), δ 1.36−0.55 (m, aliphatic). $^{195}Pt\{^1H\}$ NMR (CD_2Cl_2, 298 K): δ −4657 (t, $^1J_{P,Pt}$ = 3194 Hz, **13**), δ −3526 (dd, $^1J_{P,Pt}$ = 4246 Hz, $^2J_{P,Pt}$ = 130 Hz, **14**).

Computational Details. All calculations were carried out with Jaguar 7.5 program[32] using the density functional theory (DFT) with the B3LYP and M06 exchange-correlation functionals.[33,34] For all considered complexes, an exhaustive search of the most stable structures, including possible isomers and conformations, was carried out in gas phase using the B3LYP functional and a LACVP* basis set, consisting of the 6-31G(d) set for the main-group elements,[35] and the Hay and Wadt core valence ECP basis set of double-ζ quality for the metal atoms.[36] For the most stable structures of each complex, vibrational frequency calculations based on analytical second derivatives at the same level of theory were carried out to confirm the nature of the local minima and to compute the zero-point-energy (ZPE) and vibrational entropy corrections at 298.15 K. These structures were then reoptimized in gas phase at the M06/LACVP* level of theory.

Solvation energies were evaluated by using the Poisson−Boltzmann (PB) continuum solvent method implemented in Jaguar to simulate the THF environment (ε = 24.3 and σ = 2.262 Å).[37,38] The electronic and solvation energies of every most stable minimum were re-evaluated with single-point calculation using the larger LACV3P++**, consisting of the 6-311++G(d,p) set for the main-group elements,[39] and the Hay and Wadt core valence ECP basis set of triple-ζ quality plus one diffuse d function for the metal atoms.[36] The reaction enthalpies in solution were estimated by adding the solvation free energies to the corresponding gas phase enthalpies.

For reactions involving the formation of solid NaCl, the absolute standard enthalpy, $H°$(NaCl), and Gibbs free energy, $G°$(NaCl), of the NaCl crystal were evaluated combining the calculated Na^+ and Cl^- gas phase absolute standard enthalpies, $H°(Na^+)$ and $H°(Cl^-)$, and standard free energies, $G°(Na^+)$ and $G°(Cl^-)$, with the experimental reticular energy, $\Delta H°$(ret,exp), and absolute standard entropies, $S°$(exp), of the crystal, according to

$$H°(\mathrm{NaCl}) = H°(Na^+) + H°(Cl^-) + \Delta H°(\mathrm{ret,\ exp})$$

$$G°(\mathrm{NaCl}) = H°(\mathrm{NaCl}) - TS°(\mathrm{exp})$$

Although the B3LYP exchange correlation functional has been increasingly and successfully employed in DFT calculations in the last two decades, it does not adequately treat dispersion interactions and it has recently emerged that it may give inaccurate geometries and energies when large molecules with significant steric and hydrophobic intramolecular interactions are considered. Recent benchmark studies have shown that newly developed exchange-correlation functionals explicitly built to take into account these effects, such as M06, may give much better results.[34] For these reasons, we tested the M06 functional for the considered large trinuclear organometallic clusters to ascertain whether it could give comparable or better results than the B3LYP functional. We therefore performed benchmark calculations at both B3LYP and M06 levels on a series of $PtCo_2$ trinuclear clusters similar to those considered in this study, i.e. $[PtCo_2(CO)_7\{Ph_2PN(R)PPh_2\}]$ with R = $-(CH_2)_9CH_3$, $-(CH_2)_2S(CH_2)_5CH_3$, $-(CH_2)_2SCH_2C_6H_5$, $-C_6H_5$, for which a large amount of experimental structural and thermodynamical data (on the equilibrium between the bridged and chelate isomers) are available.[8] To save computational time and avoid convergence problems, the long n-decyl and n-hexyl chains in the cluster with the $(CH_2)_9CH_3$ and $(CH_2)_2S(CH_2)_5CH_3$ N-substituents have been replaced with a n-propyl and an ethyl group, respectively. Geometry optimizations were carried out for all complexes, and the calculated structure for $[PtCo_2(CO)_7\{Ph_2PN[(CH_2)_2SCH_2C_6H_5]$-$PPh_2\}]$, for which the X-ray structure is known, is compared with the experimental data. The overall geometry is shown in Figure 8 while the main geometrical parameters calculated at the B3LYP and M06 levels are reported together with the corresponding X-ray values in Table 3. As shown in Table 3, the M06 results are in a significantly better agreement with the X-ray data; moreover, a much better agreement is observed when the relative distances and orientation of the benzyl group with respect to the phenyl substituents on the dppa ligand are considered.

We then calculated at both levels of theory the relative stabilities of the bridged and chelated isomers of all the $[PtCo_2(CO)_7\{Ph_2PN(R)$-$PPh_2\}]$ clusters (R = $-(CH_2)_9CH_3$, $-(CH_2)_2S(CH_2)_5CH_3$, $-(CH_2)_2$-

dx.doi.org/10.1021/ic301445h | Inorg. Chem. 2012, 51, 11549−11561

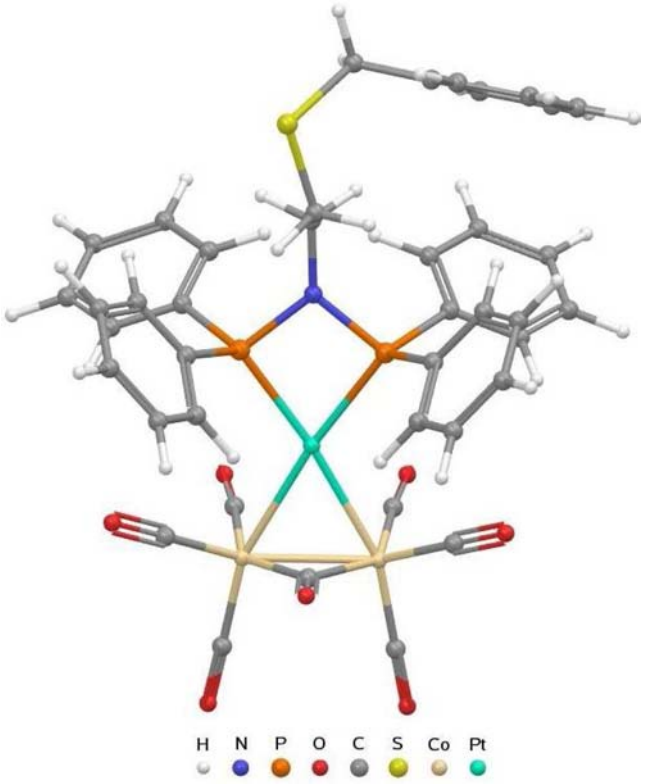

Figure 8. Geometry of $[PtCo_2(CO)_7\{Ph_2PN(R)PPh_2\}]$ (R = $-CH_2CH_2SCH_2Ph$) calculated at the M06 level.

Table 3. Main Geometrical Parameter (Angstroms for Distances and Degrees for Angles) Calculated for $[PtCo_2(CO)_7\{Ph_2PN(R)PPh_2\}]$ (R = $CH_2CH_2SCH_2Ph$) at the B3LYP and M06 Level, Compared with the Experimental XRD Values

	B3LYP	M06	experimental
Pt−Co1	2.56	2.53	2.5587(5)
Pt−Co2	2.56	2.55	2.5511(5)
Co1−Co2	2.54	2.55	2.5511(7)
Pt−P1	2.31	2.29	2.2427(9)
Pt−P2	2.31	2.29	2.2351(9)
P1−Pt−P2	72.0	71.8	71.53(3)
Co1−Pt−Co2	59.6	60.1	60.010(16)

Table 4. Comparison of Calculated and Experimental Thermodynamic Data (kcal·mol^{-1}) at 298 K for the Bridged to Chelate Isomerization of $[PtCo_2(CO)_7\{Ph_2PN(R)PPh_2\}]$ Clusters (R = $-(CH_2)_9CH_3$, $-(CH_2)_2S(CH_2)_5CH_3$, $-(CH_2)_2SCH_2C_6H_5$, and $-C_6H_5$)

	B3LYP		M06		experimental	
R	ΔH	ΔG	ΔH	ΔG	ΔH	ΔG
$(CH_2)_9CH_3$	−1.6	−4.0	−0.6	−2.8	+2.7	−0.4
$(CH_2)_2S(CH_2)_5CH_3$	−4.2	−8.1	−2.8	−6.4	+3.1	−0.4
$(CH_2)_2SCH_2C_6H_5$	−1.1	−5.3	−0.4	−2.6	+1.9	−0.3
C_6H_5	−0.8	−2.7	+0.1	−0.1	–	–

$SCH_2C_6H_5$, C_6H_5), and the results are compared with the experimental values in Table 4.

The results of both geometry optimization and relative energies of the bridged and chelated isomers clearly indicate that the M06 gives much more reliable results and therefore only this level of theory was employed in the theoretical study of the $PtMo_2$ and PtW_2 clusters.

Indeed, as shown by this comparison, the M06 calculation gave slightly exoergonic bridged to chelate isomerization free energies, only 2−3 kcal·mol^{-1} lower than the experimental values, a fairly good result if we take into account the unavoidable approximations in the modeling of the N-terminal substituents, the solvent effect, and the entropy evaluation.

■ ASSOCIATED CONTENT

Supporting Information

HRMS(−) spectrogram of **5**, MS/MS spectrogram of **4**, $^1H-^{31}P$ HMQC spectra of **4**, **5**, **10**, **11**−**12**; ^1H COSY spectra of **4**, **5**; ^1H NOESY spectra of **4**, **5**, **9**, **10**, **11**−**12**; $^{13}C\{^1H\}$ APT spectra of **4**, **5**; $^{195}Pt\{^1H\}$ NMR spectra of **4**, **5**; $^{31}P\{^1H\}$ NMR spectra of **5**, **6**, **7**, **9**, **10**, **11**−**12**, **13**−**14**; $^1H-^{195}Pt$ HMQC spectrum of **4**; calculated geometries of **4**, **11**, and **12**; free energy profile for the formation of **5** and **5***, and of **13** and **14**; Cartesian coordinates of the clusters. This material is available free of charge via the Internet at http://pubs.acs.org.

■ AUTHOR INFORMATION

Corresponding Author

*E-mail: p.mastrorilli@poliba.it (P.M.); braunstein@unistra.fr (P.B.).

Notes

The authors declare no competing financial interest.

■ ACKNOWLEDGMENTS

Italian MIUR (PRIN project no. 2009LR88XR), COST Phosphorus Science Network (PhoSciNet, project CM0802), the CNRS, and the Ministère de la Recherche (Paris) are gratefully acknowledged for financial support.

■ DEDICATION

Dedicated to Richard D. Adams, on the occasion of his 65th birthday, with our sincere congratulations

■ REFERENCES

(1) Selected review articles: (a) Puddephatt, R. J. *Chem. Soc. Rev.* **1983**, *12*, 99−127. (b) Witt, M.; Roesky, H. W. *Chem. Rev.* **1994**, *94*, 1163−1181. (c) Balakrishna, M. S.; Sreenivasa Reddy, Y.; Krishnamurthy, S. S.; Nixon, J. F.; Burckett St Laurent, J. C. T. R. *Coord. Chem. Rev.* **1994**, *129*, 1−90. (d) Mague, J. T. *J. Cluster Sci.* **1995**, *6*, 217−269. (e) Bhattacharyya, P.; Woollins, J. D. *Polyhedron* **1995**, *14*, 3367−3388. (f) Braunstein, P.; Knorr, M.; Stern, C. *Coord. Chem. Rev.* **1998**, *178*−*180*, 903−965. (g) Appleby, T.; Woollins, J. D. *Coord. Chem. Rev.* **2002**, *235*, 121−140.

(2) (a) Lee, C. L.; Yang, Y. P.; Reetting, S. J.; James, B. R.; Nelson, D. A.; Lilga, M. A. *Organometallics* **1986**, *5*, 2220−2228. (b) Barkley, J. V.; Grimshaw, J. C.; Higgins, S. J.; Hoare, P. B.; McKart, M. K.; Smith, A. K. *J. Chem. Soc., Dalton Trans.* **1995**, 2901−2908. (c) Barkley, J. V.; Ellis, M.; Higgins, S. J.; McCart, M. K. *Organometallics* **1998**, *17*, 1725−1731.

(3) Braunstein, P.; de Méric de Bellefon, C.; Lanfranchi, M.; Tiripicchio, A. *Organometallics* **1984**, *3*, 1772−1774.

(4) Braunstein, P.; Guarino, N.; de Méric de Bellefon, C.; Richert, J.-L. *Angew. Chem., Int. Ed. Engl.* **1987**, *26*, 88−89; *Angew. Chem.* **1987**, *99*, 77−79.

(5) Braunstein, P.; de Méric de Bellefon, C.; Oswald, B.; Ries, M.; Lanfranchi, M.; Tiripicchio, A. *Inorg. Chem.* **1993**, *32*, 1638−1348.

(6) (a) Bachert, I.; Bartusseck, I.; Braunstein, P.; Guillon, E.; Rosé, J.; Kickelbick, G. *J. Organomet. Chem.* **1999**, *580*, 257−264. (b) Bachert, I.; Bartusseck, I.; Braunstein, P.; Guillon, E.; Rosé, J.; Kickelbick, G. *J. Organomet. Chem.* **1999**, *588*, 144−151.

(7) Braunstein, P.; de Méric de Bellefon, C.; Oswald, B. *Inorg. Chem.* **1993**, *32*, 1649−1655.

(8) Gallo, V.; Mastrorilli, P.; Nobile, C. F.; Braunstein, P.; Englert, U. *Dalton Trans.* **2006**, 2342−2349.

(9) Bhattacharyya, B.; Sheppard, R. N.; Slawin, A. M. Z.; Williams, D. J.; Woollins, J. D. *Dalton Trans.* **1993**, 2393−2400.
(10) Throughout the paper, the calculated (exact mass) and the experimental (accurate) *m*/*z* values have been compared considering the principal ion (which gives the most intense peak) of the isotope pattern.
(11) For simplicity, throughout the paper we will specify only the lowest number of bonds separating two coupled nuclei in the symbol of the coupling constants. Thus, for example, $^{2/3}J_{P,P}$, $^{2/3}J_{P,Pt}$, or $^{2/3}J_{P,W}$ will be indicated as $^{2}J_{P,P}$, $^{2}J_{P,Pt}$, and $^{2}J_{P,W}$, respectively.
(12) Goodfellow, R. J. In *Multinuclear NMR*, Mason, J., Ed.; Plenum Press: New York, 1987, pp 521−561.
(13) Gansow, O. A.; Vernon, W. D. In *Topics in Carbon-13 NMR Spectroscopy*; Levy, G. C., Ed.; Wiley: New York, 1976; Vol. 2, pp 269−341.
(14) Band, E.; Muetterties, E. L. *Chem. Rev.* **1978**, *78*, 639−658.
(15) (a) Evans, J.; Johnson, B. F. G.; Lewis, J.; Matheson, T. W. *Chem. Commun.* **1975**, 576−577. (b) Evans, J.; Johnson, B. F. G.; Lewis, J.; Matheson, T. W.; Norton, J. R. *J. Chem. Soc., Dalton Trans.* **1978**, 626−634. (c) Alvarez, C. M.; Alvarez, M. M.; Garcìa, M. E.; Ramos, A.; Ruiz, M. A.; Graiff, C.; Tiripicchio, A. *Organometallics* **2007**, *26*, 321−331.
(16) Hashimoto, H.; Tobita, H.; Ogino, H. *Inorg. Chim. Acta* **2003**, 347−354.
(17) Chen, X.; Mann, B. E. *J. Chem. Soc., Dalton Trans.* **2000**, 2259−2266.
(18) Decker, S. A.; Donini, O.; Klobukowski, M. *J. Phys. Chem. A* **1997**, *101*, 8734−8740.
(19) Farrugia, L. J. *J. Chem. Soc., Dalton Trans.* **1997**, 1783−1792.
(20) Farrugia, L. J.; Mustoo, L. *Organometallics* **1992**, *11*, 2941−2944.
(21) Wachter, J.; Riess, J. G.; Mitschler, A. *Organometallics* **1984**, *3*, 714−722.
(22) Chen, X.; Mann, B. E. *Organometallics* **1996**, *15*, 3703−3707.
(23) Ball, R. G.; Edelmann, F.; Kiel, G. Y.; Takats, J.; Drews, R. *Organometallics* **1986**, *5*, 829−839.
(24) Marsella, J. A.; Caulton, K. G *Organometallics* **1982**, *1*, 274−279.
(25) Complexes structurally related to **6** and **7** are described in Knorr, M.; Strohmann, C. *Organometallics* **1999**, *18*, 248−257.
(26) In C_6D_6 at 298 K, the $^{31}P\{^{1}H\}$NMR spectrum of the isotopologue containing neither ^{195}Pt nor ^{183}W consists of an AB system centered at δ 70.
(27) In the case of **12**, a very weak cross peak between the two P atoms was observed in the $^{31}P\{^{1}H\}$ EXSY spectrum recorded at 298 K, with a mixing time of 0.40 s, suggesting the occurring of a (not frequent) dynamic process that does not pass through the chelate isomer.
(28) Gallo, V.; Mastrorilli, P.; Braunstein, P. unpublished results.
(29) Komine, N.; Tsutsuminai, S.; Hoh, H.; Yasuda, T.; Hirano, T.; Komiya, S. *Inorg. Chim. Acta* **2006**, *359*, 3699−3708.
(30) (a) Braunstein, P.; de Méric de Bellefon, C.; Ries, M.; Fischer, J. *Organometallics* **1988**, *7*, 332−343. (b) Braunstein, P.; de Méric de Bellefon, C.; Ries, M. *Inorg. Chem.* **1990**, *29*, 1181−1186.
(31) Braunstein, P.; Bender, R.; Jud, J. *Inorg. Synth.* **1989**, *26*, 341−350.
(32) *Jaguar*, version 6.0; Schrödinger, LLC.: New York, 2007.
(33) (a) Becke, A. D. *J. Chem. Phys.* **1993**, *98*, 5648−5652. (b) Lee, C. T.; Yang, W. T.; Parr, R. G. *Phys. Rev.* **1988**, *37*, 785−789.
(34) Zhao, Y.; Truhlar, D. G. *Theor. Chem. Acc.* **2008**, *120*, 215−241.
(35) Hehre, W. J.; Ditchfield, R.; Pople, J. A. *J. Chem. Phys.* **1972**, *56*, 2256−2261.
(36) (a) Hay, P. J.; Wadt, W. R. *J. Chem. Phys.* **1985**, *82*, 270−283. (b) Wadt, W. R.; Hay, P. J. *J. Chem. Phys.* **1985**, *82*, 284−298. (c) Hay, P. J.; Wadt, W. R. *J. Chem. Phys.* **1985**, *82*, 299−310.
(37) (a) Tomasi, J.; Persico, M. *Chem. Rev.* **1994**, *94*, 2027−2094. (b) Cramer, C. J.; Truhlar, D. G. *Chem. Rev.* **1999**, *99*, 2161−2200.
(38) (a) Tannor, D. J.; Maarten, B.; Murphy, R. B.; Friesner, R. A.; Sitkoff, D.; Nicholls, A.; Ringnalda, M. N.; Goddard, W. A., III; Honig, B. *J. Am. Chem. Soc.* **1994**, *116*, 11875−11882. (b) Maarten, B.; Kim, K.; Cortis, C.; Friesner, R. A.; Murphy, R. B.; Ringnalda, M. N.; Sitkoff, D.; Honig, B. *J. Phys. Chem.* **1996**, *100*, 11775−11788.
(39) Krishnan, R.; Binkley, J. S.; Seeger, R.; Pople, J. A. *J. Chem. Phys.* **1980**, *72*, 650−654.